

1 Sequence and structure conservation analysis of the key
2 coronavirus proteins supports the feasibility of discovering
3 broad-spectrum antiviral medications.

4 Cleber C. Melo-Filho,^a Tesia Bobrowski,^a Holli-Joi Martin,^a Zoe Sessions,^a Konstantin Popov,^b
5 Nathaniel J. Moorman,^c Ralph S. Baric,^d Eugene N. Muratov,^{a,*} Alexander Tropsha.^{a,*}

6
7 ^a Laboratory for Molecular Modeling, Division of Chemical Biology and Medicinal Chemistry, UNC
8 Eshelman School of Pharmacy, University of North Carolina, Chapel Hill, NC, 27599, USA.

9 ^b Department of Biochemistry and Biophysics, School of Medicine, University of North Carolina, Chapel
10 Hill, NC 27599, USA.

11 ^c Department of Microbiology and Immunology, School of Medicine, University of North Carolina, Chapel
12 Hill, NC, 27599, USA.

13 ^d Department of Epidemiology, Gillings School of Public Health, University of North Carolina, Chapel
14 Hill, NC, 27599, USA.

15
16 **Corresponding Authors**

17 * Address for correspondence: 331 Beard Hall, UNC Eshelman School of Pharmacy, University
18 of North Carolina, Chapel Hill, NC, 27599, USA; Telephone: (919) 966-2955; FAX: (919) 966-
19 0204; E-mail: murik@email.unc.edu; alex_tropsha@unc.edu.

20
21

22 **ABSTRACT**

23 Coronaviruses are a class of single-stranded, positive-sense RNA viruses that have caused three
24 notable outbreaks over the past two decades: Middle East respiratory syndrome–related
25 coronavirus (MERS-CoV), severe acute respiratory syndrome coronavirus (SARS-CoV), and
26 severe acute respiratory syndrome coronavirus 2 (SARS-CoV-2). All outbreaks have been
27 associated with significant morbidity and mortality. In this study, we hypothesized that conserved
28 binding sites in the key coronavirus proteins can be explored for the development of broad-
29 spectrum direct acting anti-coronaviral compounds, identified such conserved binding site residues
30 across coronaviruses, and validated our hypotheses with existing experimental data. We have
31 identified four coronaviral proteins with highly conserved binding site sequence and 3D structure
32 similarity: PL^{pro}, M^{pro}, nsp10-nsp16 complex(methyltransferase), and nsp15 endoribonuclease. We
33 have compiled all available experimental data for known antiviral medications inhibiting these
34 targets and identified compounds active against multiple coronaviruses. The identified compounds
35 representing potential broad-spectrum antivirals include: GC376, which is active against six viral
36 M^{pro} (out of six tested, as described in research literature); mycophenolic acid, which is active
37 against four viral PL^{pro} (out of four); and emetine, which is active against four viral RdRp (out of
38 four). The approach described in this study for coronaviruses, which combines the assessment of
39 sequence and structure conservation across a viral family with the analysis of accessible chemical
40 structure – antiviral activity data, can be explored for the development of broad-spectrum drugs
41 for multiple viral families.

42

43 INTRODUCTION

44 Coronaviruses are a class of single stranded, positive-sense RNA viruses that have caused
45 significant morbidity and mortality in recent years. Coronaviruses of the genus
46 *Alphacoronaviridae*, which contains some of the common cold coronaviruses, and
47 *Betacoronaviridae*, which contains the three well-known coronaviruses MERS-CoV, SARS-CoV,
48 and SARS-CoV-2, have been isolated from wildlife such as bats, palm civets, and camels.^{1,2} The
49 alphacoronaviruses HCoV-NL63 and HCoV-229E and the betacoronaviruses HCoV-OC43 and
50 HCoV-HKU1 are the endemic human coronaviruses that typically result in the common cold.²
51 These viruses usually cause only mild respiratory illness, but can result in more severe disease in
52 immunocompromised individuals, the elderly, and infants.² A third genus, including porcine delta-
53 coronavirus holds zoonotic potential, as strains have recently been identified in plasma samples of
54 three Haitian children.³

55 The noted potential for zoonotic transmission and the emergence of novel coronaviruses
56 creates an urgent need to rapidly develop new broad-spectrum antiviral therapies in addition to
57 those that currently circulate, e.g., SARS-CoV-2.^{4,5} In the previous MERS-CoV and SARS-CoV
58 outbreaks, the fatality rates were 35% and 10%, respectively, but the number of infected
59 individuals was relatively low with 2,574 and 8,422 cases, respectively.^{6,7} A striking deviation
60 from this pattern has been observed for SARS-CoV-2, which, since December 2019 and as of
61 March, 2022, has infected over 450 million people and killed over 6 million people globally.⁸⁻¹⁰
62 As the pandemic continues ravaging the world, its effects on society, poverty, the environment,
63 and the economy grow.^{11,12} Despite the desperate need for therapies, there are currently no
64 approved drugs to treat any of these coronaviruses, though several including tocilizumab,
65 sotrovimab, bamlanivimab, etesevimab, casirivimab, imdevimab, and baricitinib have been

66 approved through Emergency Use Authorization (EUA) by the FDA during the COVID-19
67 pandemic.¹³

68 Through extensive research into the mechanisms of coronavirus replication and function,
69 scientists have begun to discern important nuances concerning coronaviruses. One such variation
70 is that the host receptors for coronaviruses can differ even between genera. For instance, in the
71 genus *Betacoronavirus*, MERS-CoV uses dipeptidyl peptidase-4 (DPP4) for host cell entry
72 whereas SARS-CoV and SARS-CoV-2 use the angiotensin-converting enzyme 2 (ACE2) as their
73 host receptor.¹⁴ After binding, the spike (S) protein on the outside of the coronavirus virion must
74 be primed by host cell proteases to catalyze a conformational change that will enable its fusogenic
75 activity, thus permitting the virus to enter the host cell cytosol. This priming is typically
76 accomplished by transmembrane serine protease 2 (TMPRSS2), cathepsin L, or some other
77 cellular protease.^{14,15} Next, the two polyproteins, pp1a and pp1ab, must be translated from the
78 virion genomic RNA. These two polyproteins are cleaved by viral proteases to produce the 16 non-
79 structural proteins (nsps) essential for the replication of the coronavirus.¹⁶ This complex shares a
80 conserved S-adenosyl methionine (SAM)-binding pocket between SARS-CoV, MERS-CoV, and
81 SARS-CoV-2.¹⁷ The replicase-transcriptase complex (RTC) is composed of many of these nsps.
82 Mature virions can be formed after the viral genomic RNA buds into membranes of the
83 endoplasmic reticulum–Golgi intermediate compartment containing the viral structural proteins,
84 S, E, and M.^{16,18}

85 The nsps that constitute the RTC are tractable drug targets for coronaviruses, e.g., nsp12,
86 which encodes the RNA-dependent RNA polymerase (RdRp) domain responsible for replicating
87 viral RNA. Remdesivir, a nucleoside analog that has been approved by the FDA through an EUA,
88 has a mechanism of action that works through the inhibition of RdRp.¹⁹ Encoded by nsp15, the

89 RNA endonuclease (NendoU) is conserved among Nidovirales, the virus order containing
90 coronaviruses. The nsp10-nsp16 complex (ribose-2'-O-methyltransferase) has been implicated in
91 modulating the actions of NendoU, though much is still unknown about how coronaviruses
92 regulate the RNA cleavage activity of this protein.²⁰ Due to its unique conservation among
93 coronaviruses, NendoU is a unique target for broad-spectrum, coronavirus-specific antiviral drug
94 development. The drug Tipiracil, which is used to treat colorectal cancer, was recently shown to
95 bind within the NendoU active site and modestly inhibit SARS-CoV-2 replication in whole cell
96 assays.²¹ Tipiracil was not tested against other viruses, so it remains unknown whether it has broad-
97 spectrum activity. The nsp10-nsp16 complex principally functions to cap viral mRNAs, thereby
98 protecting them from host innate immune responses. Though it has been noted that, most likely,
99 the interface could not be targeted by small-molecule drugs due to its large area and complex
100 network of molecular interactions, in 2020 the SARS-CoV-2 nsp10-nsp16 complex bound to a
101 pan-methyltransferase inhibitor sinefungin was crystallized.²² Other viral nsps that show promise
102 as antiviral drug targets are the two proteases of coronaviruses, the papain-like protease (PL^{pro})
103 and the main protease (M^{pro}), which work to cleave transcribed polyproteins into 16 nsps with
104 distinct functions.^{16,23}

105 Given the high potential of recurrent coronavirus outbreaks, the development of broad-
106 spectrum antivirals is crucial to control both the present and future coronavirus epidemics.²⁴ A
107 database containing all known broad-spectrum antiviral compounds has been compiled at
108 <https://drugvirus.info/>.²⁵ Several compounds have demonstrated broad-spectrum antiviral activity
109 against Human Immunodeficiency Virus (HIV), Hepatitis C virus (HCV), and influenza viruses.²⁶
110 Compounds such as umifenovir, a viral fusion inhibitor, and nitazoxanide, a pyruvate ferredoxin
111 oxidoreductase enzyme inhibitor, have been and continue to be used against influenza viruses as

112 well as other viral respiratory illness.^{27,28} Other compounds are in development and trials, such as
113 GS-5734 (also known as remdesivir), a non-toxic and potent broad-spectrum antiviral against
114 endemic and zoonotic coronaviruses. This compound was found effective against SARS-CoV and
115 MERS-CoV *in vitro* as well as against bat CoVs, pre-pandemic bat CoVs, and circulating
116 contemporary human CoVs in primary human lung cells.²⁷

117 Amino acid residues constituting active sites of enzymes, especially crucial catalytic
118 residues, have a tendency to be highly conserved over evolutionary time.³⁰ A radical change in
119 those sites would likely confer a change in functionality, reducing the fitness of the virus. Thus,
120 the analysis of specific binding sites with a more focused consideration of individual proteins
121 conserved in (beta)coronaviruses may help guiding broad-spectrum antiviral discovery.^{31,32}

122 In this study, we have investigated whether homologous coronavirus proteins could be
123 exploited as targets for the development of broad-spectrum anti-coronaviral compounds. To this
124 end, we have analyzed the sequence similarity for all available coronavirus proteins. In addition,
125 we also analyzed binding site similarities for four homologous coronavirus proteins with known
126 3D structures deposited in the Protein Data Bank (PDB) including Papain-Like Protease (PL^{Pro}),
127 Main Protease (M^{Pro}), Methyltransferase (nsp10-nsp16), and Endoribonuclease (NendoU). Below
128 we review the current data about the sequence and structure conservation of these proteins across
129 coronaviruses as well as about molecules that have been tested for the activity against these
130 proteins. We provide a perspective on how the conservation analysis of viral proteins' sequence
131 and structure could support the discovery of broad-spectrum antivirals in response to future
132 coronavirus epidemics.

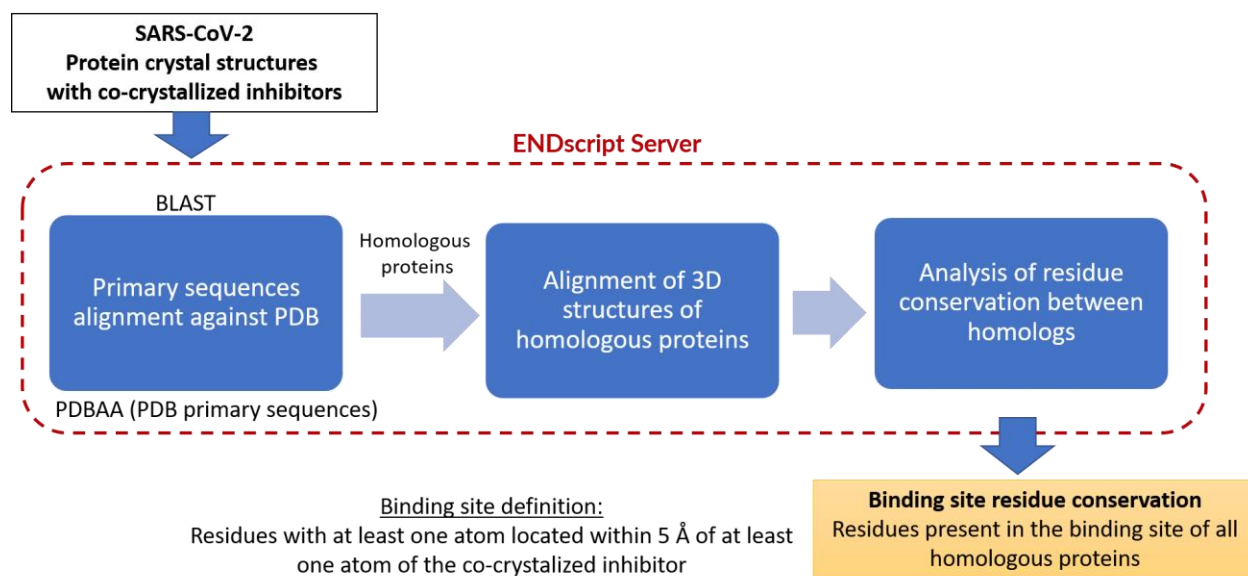
133

134

135 METHODS

136 Comparison of homologous coronavirus protein ligand binding sites

137 We analyzed the similarity between SARS-CoV-2 proteins and their related counterparts
138 from other coronaviruses, focusing specially on the comparison of ligand binding sites. SARS-
139 CoV-2 proteins were chosen as the reference and query sequences for each search. The general
140 binding site comparison workflow is presented in **Figure 1**. The details of the analysis are
141 described in the following sections.



142

143 **Figure 1.** General workflow of the protein binding sites comparison. The ENDscript server
144 (<https://endscript.ibcp.fr/ESPrpt/ENDscript/>) was employed; it is publicly accessible tool for
145 multiple sequence alignment of proteins homologous to the query, alignment of their
146 corresponding crystal structures, and coloring the query structure according to residue
147 conservation.³³

148

149 *Protein selection and collection*

150 Coronavirus proteins were selected based on the availability of their crystal structures in
151 Protein Data Bank (PDB, <http://www.rcsb.org/>).³⁴ The primary sequence of each protein was
152 obtained from UniProt.³⁵ Furthermore, since we focused on binding site comparisons, proteins
153 with co-crystallized ligands were prioritized, namely, papain-like protease (PL^{pro}), main protease

154 (M^{pro}), nsp10-nsp16 (methyltransferase), endoribonuclease (NendoU), and RNA-dependent RNA
155 polymerase (RdRP). The list of all selected proteins including their UniProt IDs and PDB codes
156 can be found in Supplemental **Tables S2-S3**.

157

158 *Homolog search and structural alignment*

159 To speed up the analysis and visualization of the primary sequence alignments, homology
160 searches, and 3D binding site alignments we used the ENDscript server.³³ This publicly accessible
161 server (<https://endscript.ibcp.fr/ESPrpt/ENDscript/>) was used to execute the following steps. 1)
162 Primary sequence alignment, using the Basic Local Alignment Search Tool (BLAST)³⁶ of a given
163 SARS-CoV-2 protein against the PDBAA database³⁷ containing all primary sequences
164 corresponding to all entries in PDB. It is important to highlight that all homologous proteins
165 identified at this stage would not necessarily cover all possible existing homologs because the
166 search was limited to the set of primary sequences with available structures in PDB (PDBAA). 2)
167 The structures of all homologs identified in the previous step were then extracted from PDB and
168 subsequently aligned both to each other and with the respective query SARS-CoV-2 protein. To
169 avoid overestimation of residue conservation due to replicate entries of the same protein from the
170 same viral species, only one representative crystal structure was considered for each protein. We
171 prioritized the structure with a co-crystallized inhibitor for comparison of the protein's ligand
172 binding sites in an inactive conformation. In the absence of a co-crystallized ligand, we chose the
173 one with the resolution. 3) A 3D structure of the query SARS-CoV-2 protein with a heat-map
174 color-coded representation of residue conservation across homologous proteins was generated. In
175 this study, the measure of conservation was based on the frequency of co-occurrence of residues
176 across homologous proteins.

177 ***Binding site similarity***

178 We focused on the conservation of experimentally defined orthosteric ligand binding sites
179 as having potential for antiviral drug development, although conservation of potential allosteric
180 binding sites could also be analyzed in a similar manner in the future. For consistency, a binding
181 site was defined as a collection of residues with at least one atom within 5Å distance from any
182 atom of the co-crystallized inhibitor.

183

184 **Primary sequence comparison of remaining proteins**

185 Primary sequences of all 26 SARS-CoV-2 proteins, including 21 proteins with no co-
186 crystallized ligands, i.e., without experimentally defined binding sites and not included in the
187 previous analysis, were used as queries for primary sequence comparisons against the “UniProtKB
188 reference proteomes plus Swiss-Prot” using BLAST³⁶ service available at Uniprot
189 (<https://www.uniprot.org/blast/>). After the search, only homologous proteins flagged as “Swiss-
190 Prot reviewed”, i.e., those that passed through a quality inspection in Swiss-Prot, were selected.
191 The resulting list of homologous proteins for each target was aligned in Clustal Omega 1.2.4³⁸
192 available at (<https://www.uniprot.org/align/>).

193

194 **RESULTS AND DISCUSSION**

195 **Binding site similarity**

196 Except for RdRp, all proteins with crystal structures containing co-crystallized inhibitors
197 returned results after submission to the ENDscript server. Despite the detection of homologs of
198 RdRp at the primary sequence level, the server did not achieve any acceptable (by internal metrics
199 that are not visible to the user) 3D alignment. Thus, two limitations are prevalent: (i) the number

200 of existing homologous proteins and their level of binding site similarity presented in this section
201 may not entirely reflect the real number of coronavirus homologous proteins because there are
202 limited PDB structures available and (ii) many mutant proteins exist, and because one
203 representative structure was chosen, this work does not reflect conservation amongst each possible
204 mutant protein for these coronaviruses. The results of this analysis are discussed below for each
205 query protein separately.

206

207 *Papain-Like Protease (PL^{pro})*

208 Eight homologous proteins of SARS-CoV-2 papain-like protease (PL^{pro}) were identified (**Table**
209 **1**). These proteins were found in coronaviruses from three different genera (*Betacoronavirus*,
210 *Gammacoronavirus*, and *Alphacoronavirus*) associated with diverse hosts (human, mice, pigs, and
211 birds). Based on primary sequence alignment, two homologous PL^{pro} with the greatest sequence
212 identity to the SARS-CoV-2 counterpart were derived from different strains of SARS-CoV and
213 presented identities of 82.54 % and 82.22% (**Table 1; Figure S1**, Supporting Information). After
214 alignment of their 3D structures, regions of high conservation (i.e., the same residue is present, in
215 the same position, in all nine homologs) were identified in the binding site defined around the co-
216 crystallized peptide-like inhibitor VIR251(**Figure 2A**).³⁹ In total, four residues in the binding site
217 of PL^{pro} from SARS-CoV-2, representing 19% of all residues in the binding site, were conserved
218 in all homologous proteins (**Table 1; Figure 2B**).

219

220

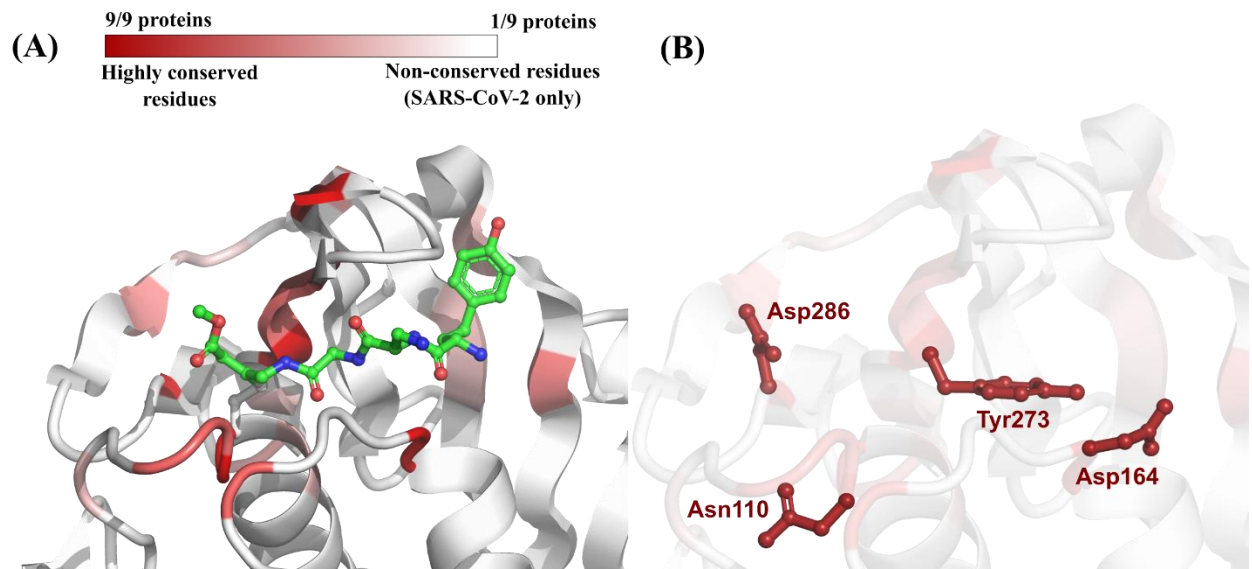
221

222

223 **Table 1.** SARS-CoV-2 PL^{pro} primary sequence identity and binding site residues conservation
 224 against all nine corresponding homologous proteins identified through ENDscript.³³
 225

PDB ID	Virus	Genus	Host	Global primary sequence identity to SARS-CoV-2 PL^{pro} (%)	SARS-CoV-2 PL^{pro} binding site residues conserved in all species
6WX4	SARS-CoV-2	<i>Betacoronavirus</i>	Human	Used as query	Asn110 Asp164 Tyr273 Asp286 (19% of all binding site residues)
3E9S	SARS-CoV	<i>Betacoronavirus</i>	Human	82.54	
4OVZ	SARS-CoV (Urbani)	<i>Betacoronavirus</i>	Human	82.22	
4P16	MERS-CoV (2c EMC/2012)	<i>Betacoronavirus</i>	Human	29.91	
4R3D	MERS-CoV (England 1)	<i>Betacoronavirus</i>	Human	29.57	
4REZ	MERS-CoV (2c Jordan-N3/2012)	<i>Betacoronavirus</i>	Human	30.03	
4X2Z	Avian Infectious Bronchitis Virus (Strain Beaudette)	<i>Gammacoronavirus</i>	Chicken	21.47	
4YPT	Murine Hepatitis Virus (strain A59)	<i>Betacoronavirus</i>	Mouse	30.00	
6L5T	Swine Acute Diarrhea Syndrome Coronavirus	<i>Alphacoronavirus</i>	Pig	20.77	

226



227

228 **Figure 2.** (A) Color-coded depiction of residue conservation at the binding site of all identified
 229 SARS-CoV-2 PL^{pro} homologous proteins. Regions in dark red represent residues with high co-
 230 occurrence among homologous proteins (i.e., nine out of nine proteins share the same residue).
 231 Regions in light red represent residues with moderate co-occurrence (i.e., between 2-8 out of nine
 232 proteins share the same residue). Regions in white represent residues with no co-occurrence (i.e.,
 233 the residue is present only in SARS-CoV-2). The protein structure used as template is the PL^{pro}
 234 from SARS-CoV-2 (PDB ID: 6WX4) co-crystallized with the peptide-like inhibitor VIR251 (in
 235 green); (B) Binding site residues of SARS-CoV-2 PL^{pro} conserved in all homologous proteins
 236 listed in **Table 1**.

237

238 *Main Protease (M^{pro})*

239 We identified eleven homologous proteins of SARS-CoV-2 main protease (M^{pro}) (**Table**
 240 **2**). These proteins were derived from the same genera of coronavirus previously identified in the
 241 PL^{pro} analysis, namely, *Betacoronavirus*, *Gammacoronavirus*, and *Alphacoronavirus*. The list of
 242 coronavirus species and associated hosts was also similar except for the Tylonycteris Bat
 243 Coronavirus HKU4, which is related to MERS-CoV.⁴⁰ Regarding primary sequence comparison,
 244 the SARS-CoV M^{pro} presented the highest identity to the SARS-CoV-2 counterpart (96.1%)
 245 followed by MERS-CoV (50.7%) (**Table 2; Figure S2**, Supporting Information). Subsequently,
 246 the 3D structural alignment of all homologs revealed regions of high conservation in the binding
 247 site defined around the co-crystallized peptide-like inhibitor N3 (**Figure 3A**).⁴¹ In total, eight

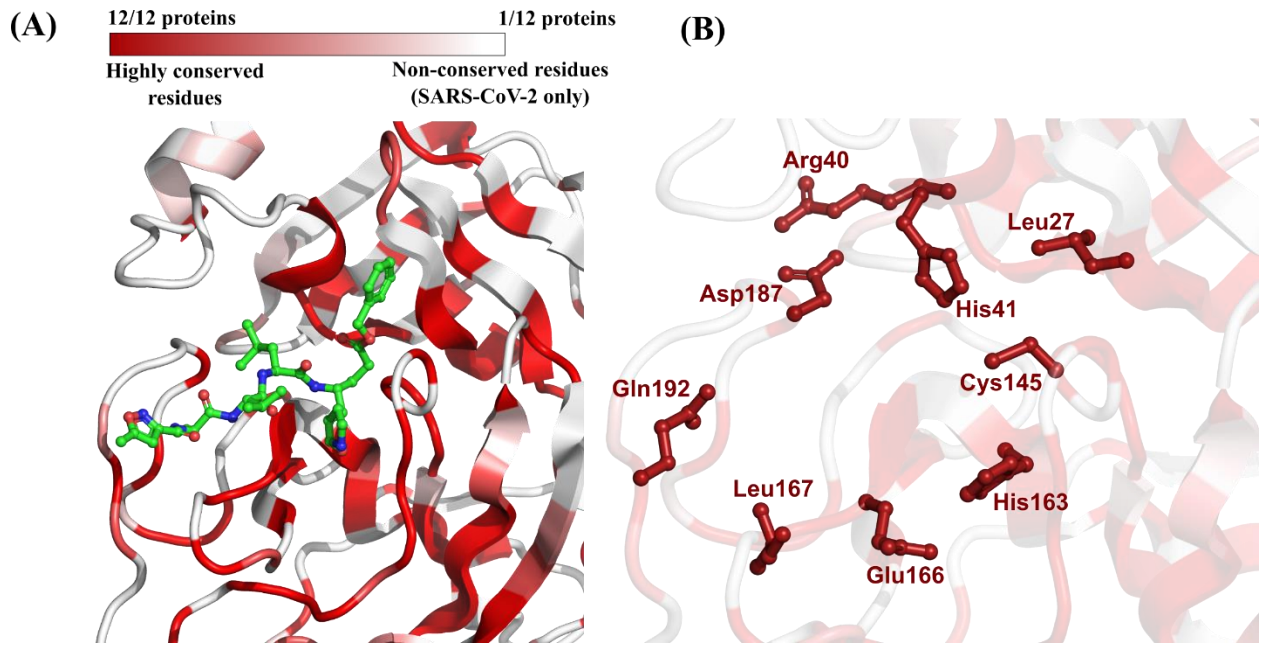
248 residues in the binding site of M^{pro} from SARS-CoV-2, which correspond to 37.5% of all residues
 249 forming the binding site, were conserved in all homologous proteins (**Table 2; Figure 3B**).

250

251 **Table 2.** SARS-CoV-2 M^{pro} primary sequence identity and binding site residues conservation
 252 against all twelve corresponding homologous proteins identified through ENDscript.³³

PDB ID	Virus	Genus	Host	Global primary sequence identity to SARS-CoV-2 M ^{pro} (%)	SARS-CoV-2 M ^{pro} binding site residues conserved in all species
6LU7	SARS-CoV-2	<i>Betacoronavirus</i>	Human	Used as query	His41 Arg40 Leu27 Asp187 Cys145 Gln192 Leu167 Glu166 His163 (37.5% of all binding site residues)
1WOF	SARS-CoV	<i>Betacoronavirus</i>	Human	96.08	
4RSP	MERS-CoV	<i>Betacoronavirus</i>	Human	50.65	
3D23	HKU1 (isolate N1)	<i>Betacoronavirus</i>	Human	49.17	
1P9S	229E	<i>Alphacoronavirus</i>	Human	39.47	
3TLO	NL63	<i>Alphacoronavirus</i>	Human	44.30	
2AMP	Transmissible Gastroenteritis Virus	<i>Alphacoronavirus</i>	Pig	44.44	
4XFQ	Porcine Epidemic diarrhea virus	<i>Alphacoronavirus</i>	Pig	44.77	
2YNA	Tylonycteris Bat Coronavirus HKU4	<i>Betacoronavirus</i>	Bat	49.68	
2Q6D	Avian Infectious Bronchitis Virus	<i>Gammacoronavirus</i>	Chicken	40.82	
4ZRO	Feline Infectious Peritonitis Virus (strain 79-1146)	<i>Alphacoronavirus</i>	Cat	44.22	
6JJJ	Murine Hepatitis Virus (strain A59)	<i>Betacoronavirus</i>	Mouse	50.33	

253



254

255 **Figure 3.** (A) Color-coded depiction of residue conservation at the binding site of all identified
 256 SARS-CoV-2 M^{pro} homologous proteins. Regions in dark red represent residues with high co-
 257 occurrence among homologous proteins (i.e., 12 out of 12 proteins share the same residue).
 258 Regions in light red represent residues with moderate co-occurrence (i.e., between 2-11 out of 12
 259 proteins share the same residue). Regions in white represent residues with no co-occurrence (i.e.,
 260 the residue is present only in SARS-CoV-2). The protein structure used as template is the M^{pro}
 261 from SARS-CoV-2 (PDB ID: 6LU7) co-crystallized with the peptide-like inhibitor N3 (in green);
 262 (B) Binding site residues of SARS-CoV-2 M^{pro} conserved in all homologous proteins.

263

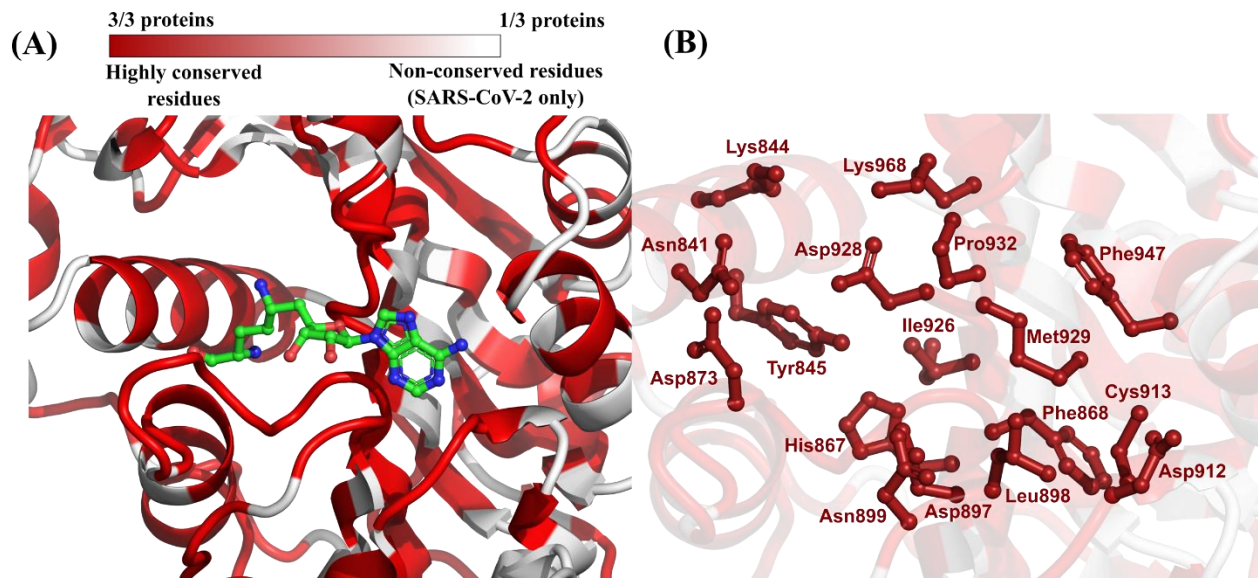
264 *nsp10-nsp16 (Methyltransferase)*

265 Only two homologous proteins of SARS-CoV-2 methyltransferase were identified in this
 266 study. These proteins correspond to the closely related SARS-CoV and MERS-CoV (strain 2c
 267 EMC/2012), both members of the *Betacoronavirus* genus that are known to infect humans and
 268 cause severe respiratory disease. The primary sequence alignment showed that SARS-CoV
 269 methyltransferase shares a high identity with its SARS-CoV-2 homolog (93.8%). The MERS-CoV
 270 homolog also shares a notable primary sequence identity with SARS-CoV-2 (66.3%) (**Table 3**;
 271 **Figure S3**, Supporting Information). Afterwards, the 3D structural alignment revealed a
 272 remarkable conservation in the binding site defined around the co-crystallized inhibitor sinefungin

273 **(Figure 4A)**.⁴² Although the high conservation could possibly be attributed to the reduced number
 274 of proteins compared in this case, it is notable how those three betacoronaviruses have important
 275 matches in binding site compositions. In total, 17 residues in the binding site of methyltransferase
 276 from SARS-CoV-2, which correspond to 77.3 % of binding site composition, were conserved in
 277 all three homologous proteins (**Table 3; Figure 4B**). Lin et al., also compared their crystal structure
 278 of the SARS-CoV-2 nsp10/nsp16 2'-O-methylase structure (PDB: 7C2I, 7C2J) to both SARS-
 279 CoV (PDB: 3R24) and MERS-CoV (PDB: 5YNM). While their analysis showed highly similar
 280 structures for SARS-CoV-2 and MERS-CoV, there were some differences observed in the RNA-
 281 binding groove of SARS-CoV which the authors attribute to a possible artifact in the structure for
 282 this region. Although the crystal structure provided by Lin et al. was not used in this study, this
 283 comparison highlights the observed conservation of both the primary sequence and secondary
 284 structure between the coronaviruses nsp10-nsp16 proteins.¹⁷

285
 286 **Table 3.** SARS-CoV-2 methyltransferase primary sequence identity and binding site residues
 287 conservation against all corresponding homologous proteins identified through ENDscript.³³
 288

PDB ID	Virus	Genus	Host	Global primary sequence identity to SARS-CoV-2 methyltransferase (%)	SARS-CoV-2 Methyltransferase binding site residues conserved in all species
6WKQ	SARS-CoV-2	<i>Betacoronavirus</i>	Human	Used as query	Lys844, Asn841, Asp873, Lys968, Asp928, Tyr845, His867, Asn899, Asp897, Ile926, Pro932, Leu898, Phe868, Met929, Phe947, Cys913, Asp912 (77.3 % of all binding site residues)
2XYR	SARS-CoV	<i>Betacoronavirus</i>	Human	93.81	
5YN5	MERS-CoV (2c EMC/2012)	<i>Betacoronavirus</i>	Human	66.33	



290

291 **Figure 4.** (A) Color-coded depiction of residue conservation at the binding site of all identified
 292 SARS-CoV-2 methyltransferase homologous proteins. Regions in dark red represent residues with
 293 high co-occurrence among homologous proteins (i.e., three out of three proteins share the same
 294 residue). Regions in light red represent residues with moderate co-occurrence (i.e., two out of three
 295 proteins share the same residue). Regions in white represent residues with no co-occurrence (i.e.,
 296 the residue is present only in SARS-CoV-2). The protein structure used as template is the nsp10-
 297 nsp16 methyltransferase from SARS-CoV-2 (PDB ID: 6WKQ) co-crystallized with the inhibitor
 298 sinefungin (in green); (B) Binding site residues of SARS-CoV-2 methyltransferase conserved in
 299 all homologous proteins.

300

301 *Endoribonuclease (NendoU)*

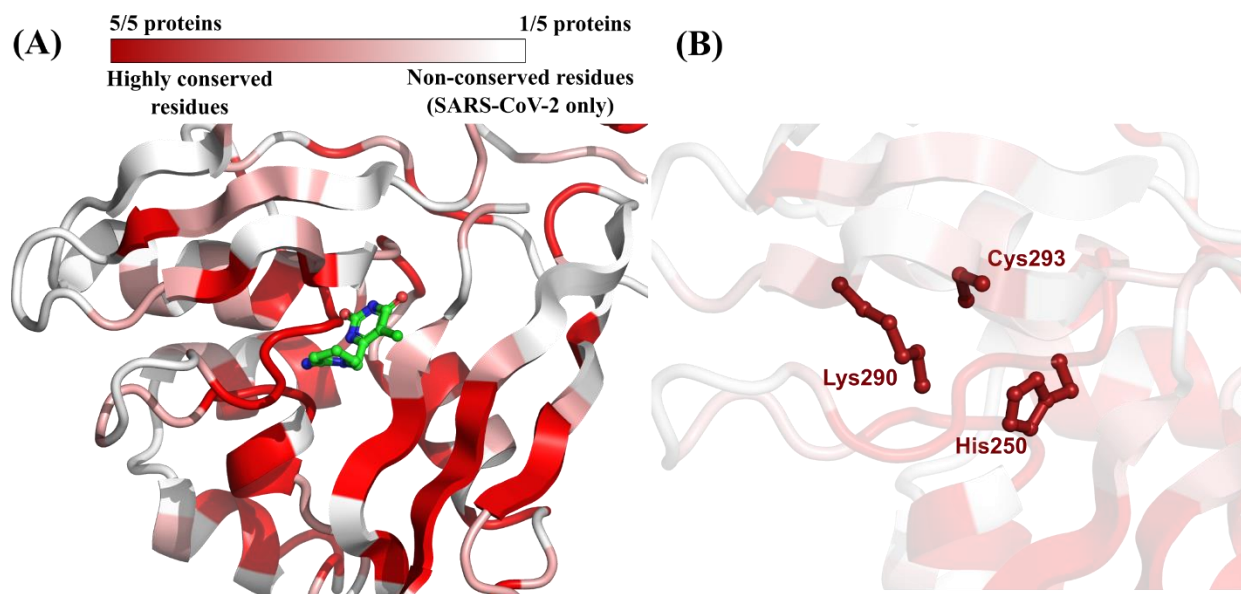
302 Four homologs of the SARS-CoV-2 endoribonuclease (NendoU) were identified: three
 303 betacoronaviruses (SARS-CoV, MERS-CoV, and Murine Hepatitis Virus) and one human
 304 alphacoronavirus (hCoV-229E). The results of primary sequence alignment showed that SARS-
 305 CoV NendoU shares a high identity (87.9%) with its SARS-CoV-2 homolog (**Table 4; Figure S4,**
 306 **Supporting Information**). After 3D structural alignment, a moderate conservation in the binding
 307 site, defined around the co-crystallized inhibitor tipiracil, was observed (**Figure 5A**).⁴³ In total,
 308 three residues in the binding site of NendoU from SARS-CoV-2, namely His250, Lys290, and

309 Cys293, representing 37.5 % of all residues in the binding site, were conserved in all five
 310 homologous proteins (**Table 4; Figure 5B**).

311
 312 **Table 4.** SARS-CoV-2 Endoribonuclease primary sequence identity and binding site residues
 313 conservation against all corresponding homologous proteins identified through ENDscript.³³
 314

PDB ID	Virus	Genus	Host	Global primary sequence identity to SARS-CoV-2 NendoU (%)	SARS-CoV-2 NendoU binding site residues conserved in all species
6WX C	SARS-CoV-2	<i>Betacoronavirus</i>	Human	Used as query	His250 Lys290 Cys293 (37.5 % of all binding site residues)
2H85	SARS-CoV	<i>Betacoronavirus</i>	Human	87.86	
5YVD	MERS-CoV	<i>Betacoronavirus</i>	Human	50.72	
4S1T	229E	<i>Alphacoronaviruses</i>	Human	42.30	
2GTH	Murine Hepatitis Virus (strain A59)	<i>Betacoronavirus</i>	Mouse	43.88	

315
 316
 317



318

319 **Figure 5.** (A) Color-coded depiction of residue conservation at the binding site of all identified
 320 SARS-CoV-2 NendoU homologous proteins. Regions in dark red represent residues with high co-
 321 occurrence among homologous proteins (i.e., five out of five proteins share the same residue).
 322 Regions in light red represent residues with moderate co-occurrence (i.e., between 2-4 out of five
 323 proteins share the same residue). Regions in white represent residues with no co-occurrence (i.e.,
 324 the residue is present only in SARS-CoV-2). The protein structure used as template is the NendoU
 325 from SARS-CoV-2 (PDB ID: 6WXC) co-crystallized with the inhibitor tipiracil (in green); (B)
 326 Binding site residues of SARS-CoV-2 NendoU conserved in all homologous proteins.

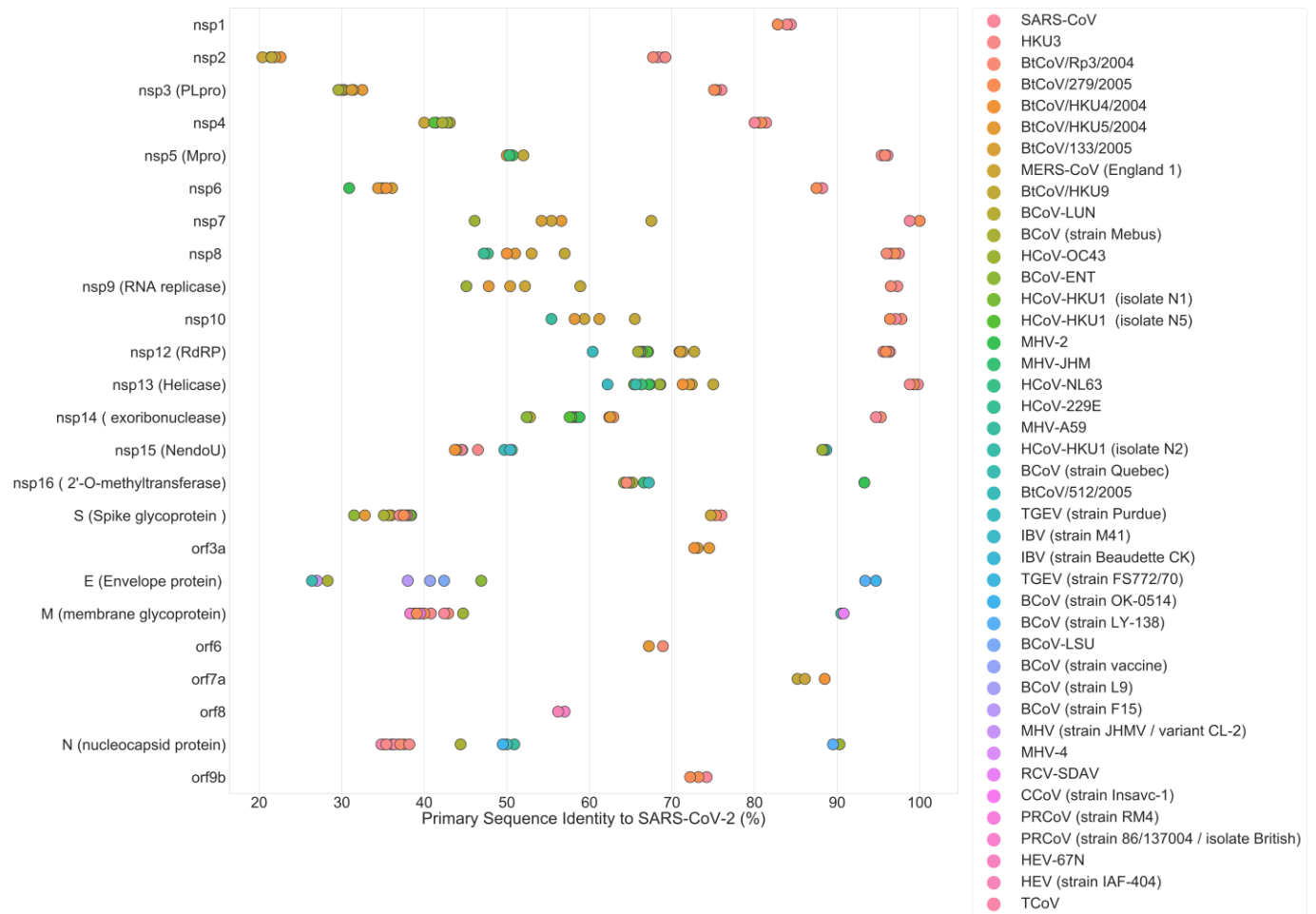
327

328 Primary sequence comparison of remaining targets

329 A total of 21 additional SARS-CoV-2 proteins, not included in the three-dimensional
 330 binding site comparisons, due to the lack of co-crystallized inhibitors, were used to search for
 331 homologs based only on their primary sequences. The results of primary sequence analysis, for 24
 332 SARS-CoV-2 proteins, are summarized in **Figure 6** and **Table S1** (Supporting Information). Two
 333 proteins did not return any results after BLAST³⁶ search (nsp11 and orf10). Protein orf10 has not
 334 yet been confirmed at the experimental level and has the lowest annotation score in the Swiss-Prot
 335 database.⁴⁴

336 Although sequence similarity is not analogous to homology, it does provide valuable
 337 insight into the possible functions of specific sequences in under-researched coronaviruses in

338 animals such as bats, rats, cows, pigs, turkeys, and others. Higher percent sequence identities are
 339 more likely to result in shared Gene Ontology (GO) annotations such as Molecular Function, which
 340 may indicate homology between proteins.⁴⁵ The high sequence identity demonstrated between
 341 some of the under-researched coronavirus sequences and that of specific proteins in SARS-CoV-
 342 2 indicates that these might also be tractable protein targets for antiviral therapies (**Figure 6**).

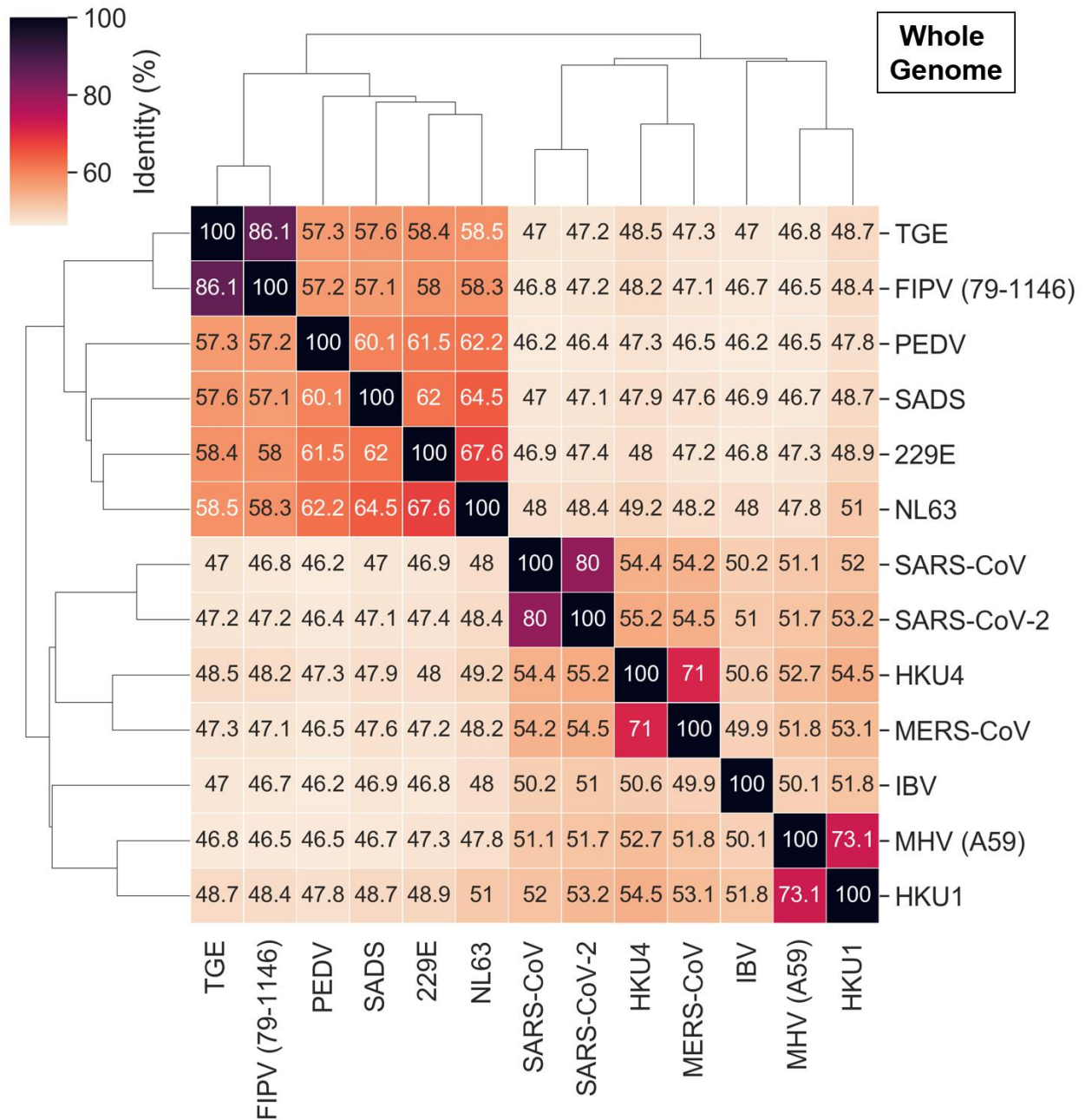


343
 344 **Figure 6.** Primary sequence identity between homologs, from various coronaviral species, and
 345 their counterparts in SARS-CoV-2 identified by BLAST.³⁶ HKU3: Bat coronavirus HKU3;
 346 BtCoV: Bat coronavirus; HCoV: Human coronavirus; MHV: Murine Hepatitis Virus; BCoV:
 347 Bovine coronavirus; TGEV: Porcine transmissible gastroenteritis coronavirus; IBV: Avian
 348 infectious bronchitis virus; RCV: Rat coronavirus; CCoV: Canine coronavirus; PRCoV: Porcine
 349 respiratory coronavirus; HEV: Porcine hemagglutinating encephalomyelitis virus; TCoV:
 350 Turkey enteric coronavirus.
 351

352 The SARS-CoV-2 pandemic has served as a reminder of the threat posed by highly
353 contagious, emerging viruses. Lack of consistent investment and research into the development of
354 antiviral agents is disappointingly common, often leaving the scientific community struggling to
355 discover therapies and create vaccines in time to treat patients and protect others once an outbreak
356 occurs (e.g., Ebola virus, Zika virus).⁴⁶ Despite this, the antiviral research prior to the COVID-19
357 pandemic enabled the scientific community to develop highly effective vaccines in record time as
358 well as quickly place remdesivir into clinical trials and receive emergency use authorization. In many
359 ways the scientific community's response to the pandemic is a success story. Establishing a similar
360 basis for successful treatments of previous and potentially similar newly emerging viruses is crucial
361 to rapidly develop both specific and broad-spectrum antivirals. In this study, we demonstrate an
362 approach to identifying conserved binding site residues across homologous viral proteins as potential
363 target sites for the discovery of broad-spectrum coronavirus antiviral drugs. The rationale for this
364 approach is illustrated by Merck's RDRP inhibitor molnupiravir that successfully passed Phase 3 of
365 clinical trials and recently gained positive FDA advisory committee vote for treatment of mild to
366 moderate COVID-19 in high risk adults. Molnupiravir case follows the same approach as discussed
367 in this study, i.e., identify conserved target (RDRP in this case), test drugs, find the one that works,
368 ensure it works across multiple strains, subject to *in vivo* experiments and clinical trials.⁴⁷⁻⁴⁹

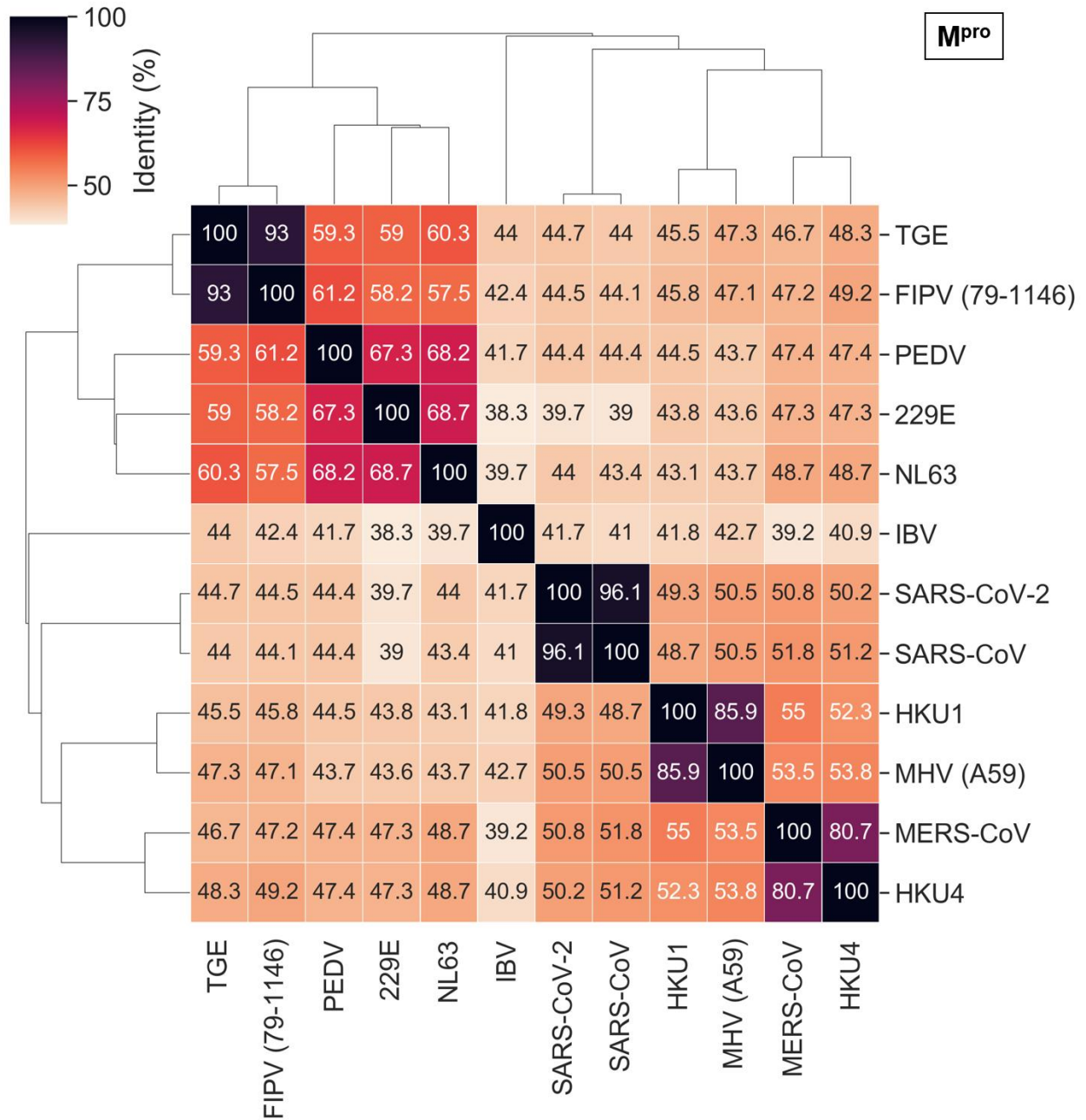
369 As detailed above, the conservation at the levels of sequence, structure, and binding sites
370 among betacoronavirus proteins was especially high for SARS-CoV-2, SARS-CoV, and MERS-
371 CoV. While perhaps not as strong, the additional binding site similarities for other coronaviruses
372 should not be disregarded. Exploring the homologs with the highest sequence and, especially,
373 binding site similarity could provide crucial insight for the development of broad-spectrum
374 antivirals, including viral outbreaks yet to come. The pairwise whole genome and M^{pro} sequence

375 similarity between the coronaviruses with available crystal structures, that we used for binding site
 376 comparison, are represented in **Figures 7 and 8**. Similar analysis for PL^{pro}, nsp10-nsp16, and
 377 NendoU proteins is depicted in **Figures S5-S7**.



378

379 **Figure 7.** Identity between all coronaviruses considered in our study based on whole genome
 380 sequence comparison.



381

382 **Figure 8.** Primary sequence comparison of M^{pro} from different coronaviruses.

383

384 Identifying conserved viral proteins can help both find similar proteins that would respond
 385 to the same (or similar) treatments as well as shed light on the key differences that might affect
 386 treatment efficacy. However, because our data compared the residue homology against the binding

387 sites of proteins in SARS-CoV-2, our set is limited in that there could be homology with other
388 coronaviruses that do not have proteins with existing crystal structures. This potential pitfall is
389 represented in our study by comparing percent sequence identity of understudied coronaviruses in
390 animals, revealing possible homologous proteins in these coronaviruses and pointing to the need
391 for the elucidation of additional viral protein crystal structures. This elucidation could be assisted
392 by the prediction of respective protein structures using recently developed computational tools
393 such as AlphaFold 2⁵⁰ that showed high accuracy in the most recent CASP competition.⁵¹

394 Analogous efforts have been made with respect to specific proteases or proteins. Prior to the
395 SARS-CoV-2 outbreak, Kim et al. concluded that the homologous M^{pro} orthosteric residues of
396 various positive-sense RNA viruses were viable candidate drug target sites for potential wide
397 spectrum treatments.⁵² In 2004, Hillisch et al., attempted homology modeling of the relatively novel
398 SARS-CoV M^{pro} but at this point they were unsuccessful and deemed the modeling insufficient.⁵³
399 Yet, in 2003, Anand et al., were able to identify considerable conservation of the SARS-CoV M^{pro}
400 binding site with that of the transmissible gastroenteritis virus, a porcine coronavirus.⁵⁴ Interestingly,
401 Yang et al. reviewed drugs that were developed for SARS-CoV and referenced the potential for M^{pro}
402 inhibitors as wide-spectrum antivirals in 2006.⁵⁵

403 The response of scientists to the SARS-CoV-2 outbreak stands as a testament to the
404 exponential advances in scientific knowledge in short periods of time. A great example of this is
405 Pfizer's development of a (relatively) selective M^{pro} inhibitor that is active against multiple
406 coronaviruses. Their compound, identified as PF-07304814, is metabolized in the body into a
407 potent M^{pro} inhibitor that has gone into Phase 1b clinical trials⁵⁶ (albeit recently Pfizer stopped
408 developing this drug for the lack of efficacy in patients).⁵⁷ To this point, many such examples of
409 M^{pro} inhibitors targeting multiple coronaviruses from our study exist (**Figure 9**) including protease

410 inhibitors of hepatitis C (boceprevir), and feline infectious peritonitis virus (GC376). Similarly,
411 inhibitors of the RNA-dependent RNA polymerase (RdRp) have shown activity against multiple
412 coronaviruses (**Figure 9**) including the approved broad-spectrum antiviral remdesivir, a nucleotide
413 analog prodrug that incorporates into the growing RNA and induces a translocation barrier to stall
414 RdRp.^{58,59} Other nucleoside analogs including molnupiravir and galidesivir have also shown to be
415 effective inhibitors of RdRp. Molnupiravir has recently successfully passed Phase 3 of clinical
416 trials and recently gained positive FDA advisory committee vote for treatment of mild to moderate
417 COVID-19 in high risk adults.⁴⁷⁻⁴⁹ Thus, further exploring nucleoside analogs that exploit
418 remdesivir's mechanism of action for multiple coronaviruses could provide additional treatment
419 options, lowering the high demand for remdesivir, therefore making treatment more affordable for
420 patients.

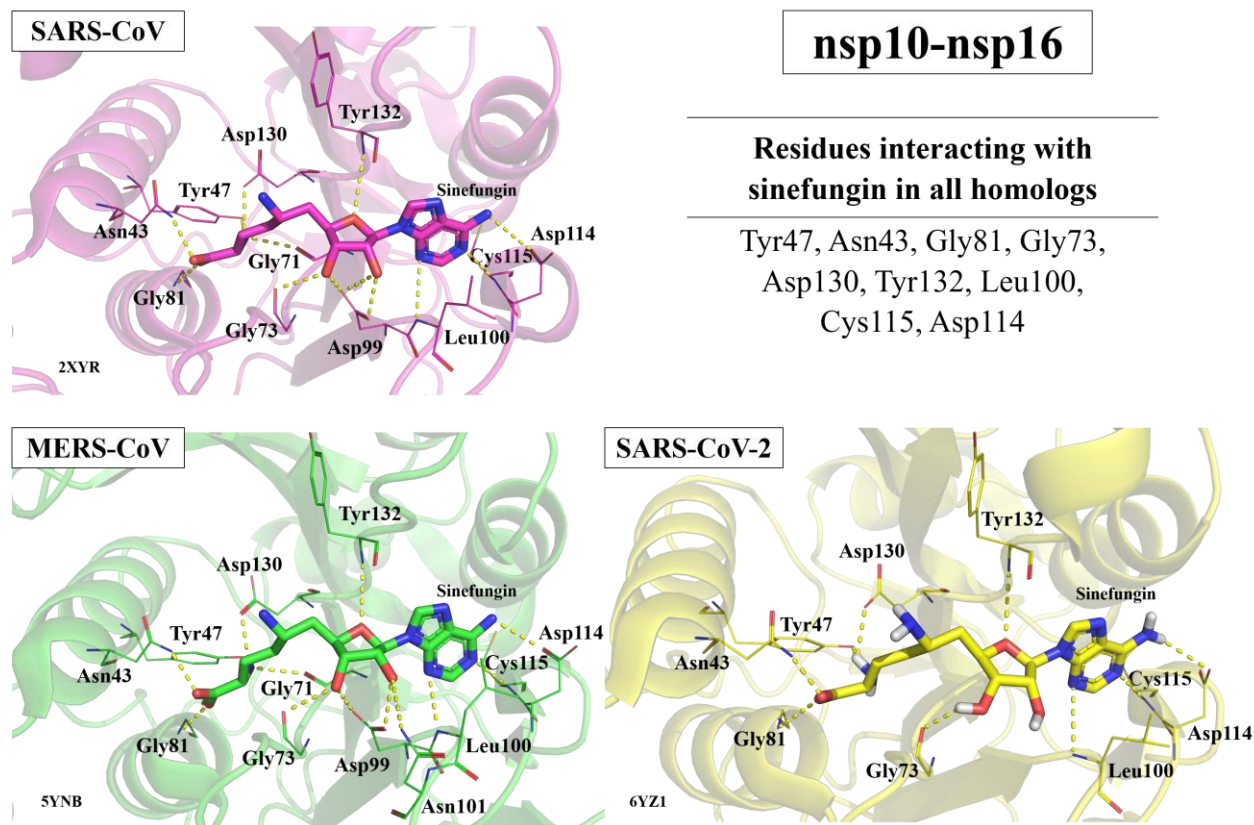
421 As mentioned above, PL^{pro} or nsp10-16 displayed homology at levels equal to or above that
422 of M^{pro}. This bodes well for the possibility of finding other drugs that will act similarly against PL^{pro}
423 or nsp10-16. While less explored than M^{pro} and RdRp, a few compounds targeting the PL^{pro}, or the
424 nsp10-16 complex of multiple coronaviruses have been identified (**Figure 9**). One interesting
425 example of a PL^{pro} inhibitor effective against SARS-CoV, MERS-CoV, and SARS-CoV-2 is
426 alcohol-aversive medication disulfiram, which is currently in Phase 2 clinical trials for the treatment
427 of SARS-CoV-2. Thiopurine analogues, like 6-mercaptopurine and 6-thioguanine also inhibit PL^{pro}
428 in SARS-CoV and MERS-CoV but have not yet been tested against PL^{pro} in SARS-CoV-2 to the
429 best of our knowledge. As for nsp10-16, the nucleoside sinefungin is effective against SARS-CoV,
430 MERS-CoV, and SARS-CoV-2. Sinefungin acts as a methyltransferase inhibitor and is effective
431 against coronaviruses due to its relation to S-adenosylmethionine (SAM), the methyl-donor required
432 for the RNA capping process which is essential for viral replication and allows coronaviruses to

433 evade the human immune system.¹⁷ Thus, although heretofore understudied as broad-spectrum
 434 coronavirus inhibitor targets, the high level of homology of both PL^{pro} and nsp10-16 as well as the
 435 proof of concept displayed by the few known inhibitors to date suggest PL^{pro} and nsp10-16 could be
 436 promising targets for future development of broad-spectrum coronavirus inhibitors. Sinefungin, for
 437 example, is a well-known inhibitor of nsp10-nsp16 protein in SARS-CoV, SARS-CoV-2, and
 438 MERS-CoV. As observed in **Figure 10**, based on available crystal structures deposited in PDB,
 439 sinefungin interacts with the same nine binding site residues in all three coronaviruses.

Compound	Target	TGE	FIPV (79-1146)	PEDV	SADS	229E	NL63	SARS-CoV	SARS-CoV-2	HKU4	MERS-CoV	IBV	MHV (A59)	HKU1
Ribavirin	RdRp			■				■	■		■			
Remdesivir					■	■	■	■	■		■			■
Galidesivir						■		■	■		■			
Emetine							■		■		■		■	
Penciclovir								■	■		■			
Homoharringtonine								■	■		■			
EIDD-1931								■	■		■			
Disulfiram	PL ^{pro}						■	■		■				
Mycophenolic Acid						■		■		■			■	
6-mercaptopurine								■	■		■			
6-thioguanine								■	■		■			
Lopinavir	M ^{pro}		■			■	■	■		■				
Nelfinavir							■	■		■				
Boceprevir						■	■	■		■				
GC376			■				■	■		■				
GC375		■	■				■	■		■				
GC373		■	■				■	■		■				
N3							■	■		■		■		
Cinanserin						■	■	■		■		■		
Calpain inhibitor II						■	■	■		■		■		
Calpain inhibitor XII						■	■	■		■		■		
Sinefungin		nsp10-nsp16						■	■		■			

■ Activity reported in literature

440
 441 **Figure 9.** Examples of inhibitors of homologous proteins (RdRp,^{60,61,70–74,62–69} PL^{pro},^{60,75–82}
 442 M^{pro},^{41,60,87–92,62,65,69,79,83–86} and nsp10-nsp16^{93–97}) targeting multiple coronaviruses. The table
 443 contains all available experimental data for drugs and compounds known to target the respective
 444 proteins and tested against different coronaviruses. TGE: Porcine transmissible gastroenteritis
 445 coronavirus; FIPV: Feline Infectious Peritonitis Virus; PEDV: Porcine Epidemic Diarrhea Virus;
 446 SADS: Swine Acute Diarrhea Syndrome Coronavirus; HKU4: Bat Coronavirus HKU4; IBV:
 447 Avian Infectious Bronchitis Virus; MHV: Murine Hepatitis Virus; HKU1: Human HKU1
 448 Coronavirus.



450

451 **Figure 10.** Interactions between sinefungin and binding site residues of nsp1-nsp16 preserved in
 452 all three homologous proteins from SARS-CoV, SARS-CoV-2, and MERS-CoV. PDB IDs:
 453 2XYR, 5YNB, 6YZ1.

454

455 Unfortunately, there are no compounds tested against all or even the majority of the viruses
 456 of interest. As represented in the **Figure 9**, each compound was tested on average against 3-4
 457 coronaviruses out of 13, ranging from 2-7 viruses per compound. SARS-CoV-2, SARS-CoV, and
 458 MERS-CoV were the most frequently tested viruses. On the other hand, no information was
 459 available on the binding of any of the 13 compounds to the viral targets for 2 of the 13 viruses.
 460 The compilation of all the available data results in a matrix with the sparsity degree of 72% which
 461 drives forth the question as to how many coronaviruses these compounds could actually work
 462 against. There were other drugs that have either been tested only in SARS-CoV-2 or negative

463 results have not been published. These drugs were not reported in this study. **Table 5** contains data
464 on compounds (including molnupiravir) that inhibited at least one of the coronavirus' homologous
465 proteins discussed above. These compounds could potentially be tested against homologs from
466 different coronavirus species. Moreover, combinations of the compounds from **Table 5** that bind
467 to protein targets responsible for different stages of viral lifecycle may be helpful in creating
468 synergistic drug combinations preserving their broad-spectrum activity.⁹⁸

469 Recently, several studies similar to ours have been published. Also exploring the
470 conservation of coronaviruses, Schapira et al.,⁹⁹ aimed to identify drug binding sites within the
471 SARS-CoV-2 proteome. Druggable binding pockets were mapped onto experimental structures of
472 SARS-CoV-2 proteins and analyzed for their conservation across all available PDB structures of
473 α - and β -coronaviruses, as well as samples from patients with SARS-CoV-2. The present study
474 complements that of Schapira et al, whereby it further explores the idea that similarities between
475 homologous coronavirus proteins could be exploited for target prioritization and the development
476 of broad-spectrum anti-coronaviral compounds, while also putting this into the context of potential
477 broad-spectrum inhibitors of conserved targets from literature. Despite the findings of both
478 Schapira et al., and this work, a recent molecular dynamics simulation study was published
479 comparing ligand-binding sites available for SARS-CoV2, SARS-CoV, and MERS-CoV M^{pro}.¹⁰⁰
480 From their simulations, the authors concluded that developing a pan-inhibitor of M^{pro} based on
481 protein conservation could be extremely challenging due to differences in the dynamics of the
482 binding sites. While this study depicts an interesting consideration in the design of future antiviral
483 medications, it is not supported by any experimental results. In contrast, we identified drugs
484 inhibiting the targets discussed in this study, carefully collected, and analyzed all known
485 experimental data on their antiviral activity and estimated their potential as broad-spectrum drugs.

486 **Table 5.** Examples of a SAR-CoV-2 EUA candidate, molnupiravir, and *in vitro* inhibitors,
487 reported in ChEMBL database, targeting proteins analyzed in our study.

Compound	Structure	Target	Virus	References
Molnupiravir		RdRP	SARS-CoV-2	47-49
CHEMBL4522602		RdRP	MERS-CoV	101
CHEMBL4544781		RdRP	MERS-CoV	101
CHEMBL2115462		RdRP	MERS-CoV	101
CHEMBL421 (Sulfasalazine)		PL ^{pro}	MERS-CoV	102
CHEMBL1368663		PL ^{pro}	MERS-CoV	102
CHEMBL1595473		PL ^{pro}	MERS-CoV	102
CHEMBL480 (Lansoprazole)		M ^{pro}	SARS-CoV-2	103
CHEMBL297453		M ^{pro}	SARS-CoV-2	103
CHEMBL1271993		M ^{pro}	SARS-CoV-2	103

489 Unfortunately, targeting highly conserved targets does not always translate into broad-
490 spectrum antiviral activity. While conservation does give a good idea of the breadth of the potential
491 spectrum of activity, there are numerous factors that create anomalies and discrepancies. As
492 described by Prichard,¹⁰⁴ there are nuances within selected molecules that could alter their activity
493 in a broad-spectrum application. Some of these include but are not limited to spectrum specificity,
494 ligand activity, binding regions of similar viruses, and post-translational modifications of proteins
495 (e.g., different phosphorylation patterns). These differences are generally enough to explain the
496 exceptions and compounds that do not work as expected.¹⁰⁴ While understanding the impact of
497 each of these nuances will be crucial to interpreting any further results derived from conservation
498 studies, it should not discourage the creation of a base of knowledge so that researchers do not
499 have to start from scratch with every new viral epidemic.¹⁰⁵

500 Collecting data as we encounter new viral threats can help in future efforts. The recent
501 emergence and spread of SARS-CoV-2 reminded the public of the momentous threat held by
502 zoonotic viruses.⁴⁶ However, SARS-CoV-2 is just one of over 250 viruses to have jumped from
503 animal to humans and caused disease.¹⁰⁶ Once a zoonotic virus jumps to humans, the threat to
504 global public health is immense. To understand these spillover events, research has been performed
505 worldwide to understand the risk of each known zoonotic virus and to predict how likely these
506 viruses are to jump to humans. One such tool called SpillOver^{106,107} was developed to identify host,
507 viral, and environmental risk factors contributing to zoonoses. SpillOver uses these risk factors to
508 provide a risk assessment score to 887 known viruses for their potential to jump to humans; the
509 first 12 of which were known to have already made the jump. Knowledge collections like these,
510 in combination with our work, are invaluable in our preparation for the next, inevitable virus to
511 jump to humans.

512 CONCLUSIONS AND PERSPECTIVES

513

514 Exploring the conservation between homologous coronavirus proteins is a valuable
515 strategy for drug target selection that could assist the development of broad-spectrum
516 anti(corona)viral compounds. We analyzed the primary sequence similarity between all known
517 SARS-CoV-2 proteins and their homologs from several human and animal coronaviruses.
518 Furthermore, we investigated 3D binding site similarities, using the ENDscript server, between
519 four SARS-CoV-2 proteins and their several homologs with three-dimensional structures available
520 in the PDB: Papain-Like Protease (PL^{pro}), Main Protease (M^{pro}), Methyltransferase (nsp10-nsp16),
521 and Endoribonuclease (NendoU). All the aforementioned proteins presented important binding site
522 conservation between SARS-CoV-2 and different human and animal coronaviruses. It is important
523 to highlight that all results of the binding site conservation analysis are limited by the availability
524 of the corresponding homologous protein structures in PDB. To demonstrate the potential of
525 exploring conserved homologous proteins for the development of broad-spectrum antivirals, we
526 found several examples of bioactive compounds and approved drugs, known to inhibit those
527 proteins, with reported activity against different animal and human coronaviruses. Some examples
528 include the RdRp inhibitor remdesivir, the PL^{pro} inhibitor disulfiram, and the nsp10-nsp16
529 inhibitor sinefungin.

530 Examining the homology of ligand binding sites in coronavirus proteins could provide an
531 immense support in searching for broad spectrum direct antiviral agents as novel viruses continue
532 to emerge. With this goal in mind, initiatives such as NIH's Antiviral Program for Pandemics¹⁰⁸
533 and READDI (Rapidly Emerging Antiviral Drug Development Initiative) at UNC Chapel Hill¹⁰⁹
534 are working to develop broad-spectrum antivirals and bring them to phase I/II clinical trials so they

535 are readily available for future viral outbreaks.¹¹⁰ This way, the scientific community does not
536 have to start *ex nihilo* in regard to antiviral drug development and may already have a head start
537 on managing outbreaks before they reach pandemic levels.¹¹⁰

538 One major advantage of surveying conservation is the ability to consider individual protein
539 targets. In doing so, the common proteins responsible for different viral functions, such as
540 replication, can be targeted and applied across a greater number of viruses. As opposed to targeting
541 viral structural proteins (which may be more important targets for vaccine development), targeting
542 replication proteins for small molecule therapies in homologous binding sites should be evaluated
543 in a more nuanced study to determine if they may be pertinent in the search for both selective and
544 broad-spectrum inhibitors.

545 Moving forward, the next step would be to attempt to compare more homologs within the
546 *Coronaviridae* as well as potentially moving outside this family. While we did this on a small
547 scale, more expansive research should be done. Targeting common host proteins and pathways
548 involved in viral entry and replication is another potential strategy for broad-spectrum antivirals
549 design (including the combination therapy), e.g., exploring the link between both T-cell immunity
550 in SARS-CoV and SARS-CoV-2 patients as well as the shared binding to the ACE2 receptor that
551 could provide a potential therapeutic overlap.¹¹¹⁻¹¹³

552 In summary, we note that finding chemicals active against highly conserved targets in
553 laboratory tests does not always translate into new broad-spectrum antivirals. However, our studies
554 suggest that this strategy could result in new treatments both for current and future viral epidemics
555 and therefore the protein targets that contain conserved sequence and at least partially conserved
556 binding sites should continue to be explored for the discovery of broad-spectrum direct antivirals.

557

558 **Associated Content**

559 Supporting information includes figures of the primary sequence alignment of Mpro, PLpro,
560 nsp10-nsp16 (methyltransferase), and NendoU. A table with primary sequence comparison results
561 for all 26 SARS-CoV-2 proteins against their homologs is also provided.

562 **Acknowledgements**

563 This study was supported in part by NIH grants R01GM140154 and 1OT2TR003441 and RO1
564 AI108197 (to RSB).

565 **Conflicts of Interest**

566 AT and ENM are co-founders of Predictive, LLC, which develops computational methodologies
567 and software for toxicity prediction. All other authors declare they have nothing to disclose.

568 **References**

- 569 (1) Monchatre-Leroy, E.; Boué, F.; Boucher, J.-M.; Renault, C.; Moutou, F.; Ar Gouilh, M.;
570 Umhang, G. Identification of Alpha and Beta Coronavirus in Wildlife Species in France:
571 Bats, Rodents, Rabbits, and Hedgehogs. *Viruses* **2017**, *9* (12), 364.
572 <https://doi.org/10.3390/v9120364>.
- 573 (2) Corman, V. M.; Muth, D.; Niemeyer, D.; Drosten, C. Hosts and Sources of Endemic Human
574 Coronaviruses. In *Advances in Virus Research*; 2018; pp 163–188.
575 <https://doi.org/10.1016/bs.aivir.2018.01.001>.
- 576 (3) Lednicky, J. A.; Tagliamonte, M. S.; White, S. K.; Elbadry, M. A.; Alam, M. M.;
577 Stephenson, C. J.; Bonny, T. S.; Loeb, J. C.; Telisma, T.; Chavannes, S.; Ostrov, D. A.;
578 Mavian, C.; De Rochars, V. M. B.; Salemi, M.; Morris, J. G. Emergence of Porcine Delta-
579 Coronavirus Pathogenic Infections among Children in Haiti through Independent Zoonoses
580 and Convergent Evolution. *medRxiv Prepr. Serv. Heal. Sci.* **2021**.
581 <https://doi.org/10.1101/2021.03.19.21253391>.
- 582 (4) Menachery, V. D.; Yount, B. L.; Debbink, K.; Agnihothram, S.; Gralinski, L. E.; Plante, J.
583 A.; Graham, R. L.; Scobey, T.; Ge, X. Y.; Donaldson, E. F.; Randell, S. H.; Lanzavecchia,
584 A.; Marasco, W. A.; Shi, Z. L.; Baric, R. S. A SARS-like Cluster of Circulating Bat
585 Coronaviruses Shows Potential for Human Emergence. *Nat. Med.* **2015**, *21* (12), 1508–
586 1513. <https://doi.org/10.1038/nm.3985>.
- 587 (5) Graham, R. L.; Baric, R. S. SARS-CoV-2: Combating Coronavirus Emergence. *Immunity*
588 **2020**, *52* (5), 734–736. <https://doi.org/10.1016/j.immuni.2020.04.016>.
- 589 (6) MERS situation update, June 2021 <http://www.emro.who.int/health-topics/mers-cov/mers->

- 590 outbreaks.html (accessed Oct 5, 2021).
- 591 (7) SARS [http://www.emro.who.int/health-topics/severe-acute-respiratory-](http://www.emro.who.int/health-topics/severe-acute-respiratory-syndrome/introduction.html)
592 [syndrome/introduction.html](http://www.emro.who.int/health-topics/severe-acute-respiratory-syndrome/introduction.html) (accessed Oct 5, 2021).
- 593 (8) Dong, E.; Du, H.; Gardner, L. An Interactive Web-Based Dashboard to Track COVID-19
594 in Real Time. *Lancet Infect. Dis.* **2020**, *20* (5), 533–534. [https://doi.org/10.1016/S1473-](https://doi.org/10.1016/S1473-3099(20)30120-1)
595 [3099\(20\)30120-1](https://doi.org/10.1016/S1473-3099(20)30120-1).
- 596 (9) COVID-19 Dashboard by the Center for Systems Science and Engineering (CSSE) at Johns
597 Hopkins <https://coronavirus.jhu.edu/map.html> (accessed Oct 5, 2021).
- 598 (10) WHO Coronavirus (COVID-19) Dashboard <https://covid19.who.int/> (accessed Oct 5,
599 2021).
- 600 (11) Saladino, V.; Algeri, D.; Auriemma, V. The Psychological and Social Impact of Covid-19:
601 New Perspectives of Well-Being. *Front. Psychol.* **2020**, *11* (October), 1–6.
602 <https://doi.org/10.3389/fpsyg.2020.577684>.
- 603 (12) Chakraborty, I.; Maity, P. COVID-19 Outbreak: Migration, Effects on Society, Global
604 Environment and Prevention. *Sci. Total Environ.* **2020**, *728*, 138882.
605 <https://doi.org/10.1016/j.scitotenv.2020.138882>.
- 606 (13) Coronavirus Disease 2019 (COVID-19) EUA Information
607 [https://www.fda.gov/emergency-preparedness-and-response/mcm-legal-regulatory-and-](https://www.fda.gov/emergency-preparedness-and-response/mcm-legal-regulatory-and-policy-framework/emergency-use-authorization# covid19euas)
608 [policy-framework/emergency-use-authorization# covid19euas](https://www.fda.gov/emergency-preparedness-and-response/mcm-legal-regulatory-and-policy-framework/emergency-use-authorization# covid19euas) (accessed Oct 5, 2021).
- 609 (14) Fehr, A. R.; Perlman, S. Coronaviruses: An Overview of Their Replication and
610 Pathogenesis. In *Coronaviruses: Methods and Protocols*; Maier, H. J., Bickerton, E.,
611 Britton, P., Eds.; Methods in Molecular Biology; Springer New York: New York, NY, 2015;
612 Vol. 1282, pp 1–23. https://doi.org/10.1007/978-1-4939-2438-7_1.
- 613 (15) Hoffmann, M.; Hofmann-Winkler, H.; Pöhlmann, S. Priming Time: How Cellular Proteases
614 Arm Coronavirus Spike Proteins. *Act. Viruses by Host Proteases* **2018**, *71*.
615 https://doi.org/10.1007/978-3-319-75474-1_4.
- 616 (16) Astuti, I.; Ysrafil. Severe Acute Respiratory Syndrome Coronavirus 2 (SARS-CoV-2): An
617 Overview of Viral Structure and Host Response. *Diabetes Metab. Syndr. Clin. Res. Rev.*
618 **2020**, *14* (4), 407–412. <https://doi.org/10.1016/j.dsx.2020.04.020>.
- 619 (17) Lin, S.; Chen, H.; Ye, F.; Chen, Z.; Yang, F.; Zheng, Y.; Cao, Y.; Qiao, J.; Yang, S.; Lu, G.
620 Crystal Structure of SARS-CoV-2 Nsp10/Nsp16 2'-O-Methylase and Its Implication on
621 Antiviral Drug Design. *Signal Transduct. Target. Ther.* **2020**, *5* (1), 131.
622 <https://doi.org/10.1038/s41392-020-00241-4>.
- 623 (18) V'kovski, P.; Kratzel, A.; Steiner, S.; Stalder, H.; Thiel, V. Coronavirus Biology and
624 Replication: Implications for SARS-CoV-2. *Nat. Rev. Microbiol.* **2021**, *19* (3), 155–170.
625 <https://doi.org/10.1038/s41579-020-00468-6>.
- 626 (19) Shannon, A.; Le, N. T. T.; Selisko, B.; Eydoux, C.; Alvarez, K.; Guillemot, J. C.; Decroly,
627 E.; Peersen, O.; Ferron, F.; Canard, B. Remdesivir and SARS-CoV-2: Structural
628 Requirements at Both Nsp12 RdRp and Nsp14 Exonuclease Active-Sites. *Antiviral Res.*

- 629 **2020**, 178 (March), 104793. <https://doi.org/10.1016/j.antiviral.2020.104793>.
- 630 (20) Ricagno, S.; Egloff, M.-P.; Ulferts, R.; Coutard, B.; Nurizzo, D.; Campanacci, V.;
631 Cambillau, C.; Ziebuhr, J.; Canard, B. Crystal Structure and Mechanistic Determinants of
632 SARS Coronavirus Nonstructural Protein 15 Define an Endoribonuclease Family. *Proc.*
633 *Natl. Acad. Sci.* **2006**, 103 (32), 11892–11897. <https://doi.org/10.1073/pnas.0601708103>.
- 634 (21) Kim, Y.; Wower, J.; Maltseva, N.; Chang, C.; Jedrzejczak, R.; Wilamowski, M.; Kang, S.;
635 Nicolaescu, V.; Randall, G.; Michalska, K.; Joachimiak, A. Tipiracil Binds to Uridine Site
636 and Inhibits Nsp15 Endoribonuclease NendoU from SARS-CoV-2. *Commun. Biol.* **2021**, 4
637 (1), 193. <https://doi.org/10.1038/s42003-021-01735-9>.
- 638 (22) Krafcikova, P.; Silhan, J.; Nencka, R.; Boura, E. Structural Analysis of the SARS-CoV-2
639 Methyltransferase Complex Involved in RNA Cap Creation Bound to Sinefungin. *Nat.*
640 *Commun.* **2020**, 11 (1), 3717. <https://doi.org/10.1038/s41467-020-17495-9>.
- 641 (23) Zumla, A.; Chan, J. F. W.; Azhar, E. I.; Hui, D. S. C.; Yuen, K.-Y. Coronaviruses — Drug
642 Discovery and Therapeutic Options. *Nat. Rev. Drug Discov.* **2016**, 15 (5), 327–347.
643 <https://doi.org/10.1038/nrd.2015.37>.
- 644 (24) Totura, A. L.; Bavari, S. Broad-Spectrum Coronavirus Antiviral Drug Discovery. *Expert*
645 *Opin. Drug Discov.* **2019**, 14 (4), 397–412.
646 <https://doi.org/10.1080/17460441.2019.1581171>.
- 647 (25) Andersen, P. I.; Ianevski, A.; Lysvand, H.; Vitkauskienė, A.; Oksenysh, V.; Bjørås, M.;
648 Telling, K.; Lutsar, I.; Dumpis, U.; Irie, Y.; Tenson, T.; Kantele, A.; Kainov, D. E.
649 Discovery and Development of Safe-in-Man Broad-Spectrum Antiviral Agents. *Int. J.*
650 *Infect. Dis.* **2020**, 93, 268–276. <https://doi.org/10.1016/j.ijid.2020.02.018>.
- 651 (26) Vigant, F.; Santos, N. C.; Lee, B. Broad-Spectrum Antivirals against Viral Fusion. *Nat. Rev.*
652 *Microbiol.* **2015**, 13 (7), 426–437. <https://doi.org/10.1038/nrmicro3475>.
- 653 (27) Boriskin, Y.; Leneva, I.; Pecheur, E.-I.; Polyak, S. Arbidol: A Broad-Spectrum Antiviral
654 Compound That Blocks Viral Fusion. *Curr. Med. Chem.* **2008**, 15 (10), 997–1005.
655 <https://doi.org/10.2174/092986708784049658>.
- 656 (28) Rossignol, J.-F. Nitazoxanide: A First-in-Class Broad-Spectrum Antiviral Agent. *Antiviral*
657 *Res.* **2014**, 110, 94–103. <https://doi.org/10.1016/j.antiviral.2014.07.014>.
- 658 (29) Sheahan, T. P.; Sims, A. C.; Graham, R. L.; Menachery, V. D.; Gralinski, L. E.; Case, J. B.;
659 Leist, S. R.; Pyrc, K.; Feng, J. Y.; Trantcheva, I.; Bannister, R.; Park, Y.; Babusis, D.;
660 Clarke, M. O.; Mackman, R. L.; Spahn, J. E.; Palmiotti, C. A.; Siegel, D.; Ray, A. S.; Cihlar,
661 T.; Jordan, R.; Denison, M. R.; Baric, R. S. Broad-Spectrum Antiviral GS-5734 Inhibits
662 Both Epidemic and Zoonotic Coronaviruses. *Sci. Transl. Med.* **2017**, 9 (396), eaal3653.
663 <https://doi.org/10.1126/scitranslmed.aal3653>.
- 664 (30) Jack, B. R.; Meyer, A. G.; Echave, J.; Wilke, C. O. Functional Sites Induce Long-Range
665 Evolutionary Constraints in Enzymes. *PLoS Biol.* **2016**, 14 (5), 1–23.
666 <https://doi.org/10.1371/journal.pbio.1002452>.
- 667 (31) Li, F. Structure, Function, and Evolution of Coronavirus Spike Proteins. *Annu. Rev. Virol.*
668 **2016**, 3 (1), 237–261. <https://doi.org/10.1146/annurev-virology-110615-042301>.

- 669 (32) Tilocca, B.; Soggiu, A.; Sanguinetti, M.; Musella, V.; Britti, D.; Bonizzi, L.; Urbani, A.;
670 Roncada, P. Comparative Computational Analysis of SARS-CoV-2 Nucleocapsid Protein
671 Epitopes in Taxonomically Related Coronaviruses. *Microbes Infect.* **2020**, *22* (4–5), 188–
672 194. <https://doi.org/10.1016/j.micinf.2020.04.002>.
- 673 (33) Robert, X.; Gouet, P. Deciphering Key Features in Protein Structures with the New
674 ENDscript Server. *Nucleic Acids Res.* **2014**, *42* (W1), W320–W324.
675 <https://doi.org/10.1093/nar/gku316>.
- 676 (34) Berman, H. M. The Protein Data Bank. *Nucleic Acids Res.* **2000**, *28* (1), 235–242.
677 <https://doi.org/10.1093/nar/28.1.235>.
- 678 (35) Bateman, A. UniProt: A Worldwide Hub of Protein Knowledge. *Nucleic Acids Res.* **2019**,
679 *47* (D1), D506–D515. <https://doi.org/10.1093/nar/gky1049>.
- 680 (36) Altschul, S. F.; Gish, W.; Miller, W.; Myers, E. W.; Lipman, D. J. Basic Local Alignment
681 Search Tool. *J. Mol. Biol.* **1990**, *215* (3), 403–410. [https://doi.org/10.1016/S0022-2836\(05\)80360-2](https://doi.org/10.1016/S0022-2836(05)80360-2).
- 683 (37) The BLAST Databases. <https://ftp.ncbi.nlm.nih.gov/blast/documents/blastdb.html>
684 (accessed Feb 4, 2021).
- 685 (38) Sievers, F.; Wilm, A.; Dineen, D.; Gibson, T. J.; Karplus, K.; Li, W.; Lopez, R.; McWilliam,
686 H.; Remmert, M.; Söding, J.; Thompson, J. D.; Higgins, D. G. Fast, Scalable Generation of
687 High-quality Protein Multiple Sequence Alignments Using Clustal Omega. *Mol. Syst. Biol.*
688 **2011**, *7* (1), 1–6. <https://doi.org/10.1038/msb.2011.75>.
- 689 (39) Rut, W.; Lv, Z.; Zmudzinski, M.; Patchett, S.; Nayak, D.; Snipas, S. J.; El Oualid, F.; Huang,
690 T. T.; Bekes, M.; Drag, M.; Olsen, S. K. Activity Profiling and Structures of Inhibitor-
691 Bound SARS-CoV-2-PLpro Protease Provides a Framework for Anti-COVID-19 Drug
692 Design. *bioRxiv Prepr. Serv. Biol.* **2020**, 1–18. <https://doi.org/10.1101/2020.04.29.068890>.
- 693 (40) Lau, S. K. P.; Li, K. S. M.; Tsang, A. K. L.; Lam, C. S. F.; Ahmed, S.; Chen, H.; Chan, K.;
694 Woo, P. C. Y.; Yuen, K. Genetic Characterization of Betacoronavirus Lineage C Viruses in
695 Bats Reveals Marked Sequence Divergence in the Spike Protein of Pipistrellus Bat
696 Coronavirus HKU5 in Japanese Pipistrelle : Implications for the Origin of the Novel Middle
697 East Respiratory. **2013**, *87* (15), 8638–8650. <https://doi.org/10.1128/JVI.01055-13>.
- 698 (41) Jin, Z.; Du, X.; Xu, Y.; Deng, Y.; Liu, M.; Zhao, Y.; Zhang, B.; Li, X.; Zhang, L.; Peng, C.;
699 Duan, Y.; Yu, J.; Wang, L.; Yang, K.; Liu, F.; Jiang, R.; Yang, X.; You, T.; Liu, X.; Yang,
700 X.; Bai, F.; Liu, H.; Liu, X.; Guddat, L. W.; Xu, W.; Xiao, G.; Qin, C.; Shi, Z.; Jiang, H.;
701 Rao, Z.; Yang, H. Structure of Mpro from SARS-CoV-2 and Discovery of Its Inhibitors.
702 *Nature* **2020**, *582* (7811), 289–293. <https://doi.org/10.1038/s41586-020-2223-y>.
- 703 (42) RCSB PDB - 6WKQ: 1.98 Angstrom Resolution Crystal Structure of NSP16-NSP10
704 Heterodimer from SARS-CoV-2 in Complex with Sinefungin
705 <https://www.rcsb.org/structure/6WKQ> (accessed Sep 17, 2020).
- 706 (43) RCSB PDB - 6WXC: Crystal Structure of NSP15 Endoribonuclease from SARS CoV-2 in
707 the Complex with potential repurposing drug Tipiracil
708 <https://www.rcsb.org/structure/6WXC> (accessed Sep 23, 2020).

- 709 (44) Apweiler, R.; Bairoch, A.; Wu, C. H.; Barker, W. C.; Boeckmann, B.; Ferro, S.; Gasteiger,
710 E.; Huang, H.; Lopez, R.; Magrane, M.; Martin, M. J.; Natale, D. a; O'Donovan, C.;
711 Redaschi, N.; Yeh, L.-S. L. UniProt: The Universal Protein Knowledgebase. *Nucleic Acids*
712 *Res.* **2004**, 32 (Database issue), D115-9.
- 713 (45) Joshi, T.; Xu, D. Quantitative Assessment of Relationship between Sequence Similarity and
714 Function Similarity. *BMC Genomics* **2007**, 8 (1), 222. [https://doi.org/10.1186/1471-2164-](https://doi.org/10.1186/1471-2164-8-222)
715 8-222.
- 716 (46) Bobrowski, T.; Melo-Filho, C. C.; Korn, D.; Alves, V. M.; Popov, K. I.; Auerbach, S.;
717 Schmitt, C.; Moorman, N. J.; Muratov, E. N.; Tropsha, A. Learning from History: Do Not
718 Flatten the Curve of Antiviral Research! *Drug Discov. Today* **2020**, 00 (00), 1–10.
719 <https://doi.org/10.1016/j.drudis.2020.07.008>.
- 720 (47) Fischer, W.; Eron, J. J.; Holman, W.; Cohen, M. S.; Fang, L.; Szewczyk, L. J.; Sheahan, T.
721 P.; Baric, R.; Mollan, K. R.; Wolfe, C. R.; Duke, E. R.; Azizad, M. M.; Borroto-Esoda, K.;
722 Wohl, D. A.; Loftis, A. J.; Alabanza, P.; Lipansky, F.; Painter, W. P. Molnupiravir, an Oral
723 Antiviral Treatment for COVID-19. *medRxiv Prepr. Serv. Heal. Sci.* **2021**.
724 <https://doi.org/10.1101/2021.06.17.21258639>.
- 725 (48) Kabinger, F.; Stiller, C.; Schmitzová, J.; Dienemann, C.; Kocic, G.; Hillen, H. S.;
726 Höbartner, C.; Cramer, P. Mechanism of Molnupiravir-Induced SARS-CoV-2 Mutagenesis.
727 *Nat. Struct. Mol. Biol.* **2021**, 28 (9), 740–746. [https://doi.org/10.1038/s41594-021-00651-](https://doi.org/10.1038/s41594-021-00651-0)
728 0.
- 729 (49) Willyard, C. How Antiviral Pill Molnupiravir Shot Ahead in the COVID Drug Hunt. *Nature*
730 **2021**. <https://doi.org/10.1038/d41586-021-02783-1>.
- 731 (50) Jumper, J.; Evans, R.; Pritzel, A.; Green, T.; Figurnov, M.; Ronneberger, O.;
732 Tunyasuvunakool, K.; Bates, R.; Žídek, A.; Potapenko, A.; Bridgland, A.; Meyer, C.; Kohl,
733 S. A. A.; Ballard, A. J.; Cowie, A.; Romera-Paredes, B.; Nikolov, S.; Jain, R.; Adler, J.;
734 Back, T.; Petersen, S.; Reiman, D.; Clancy, E.; Zielinski, M.; Steinegger, M.; Pacholska,
735 M.; Berghammer, T.; Bodenstein, S.; Silver, D.; Vinyals, O.; Senior, A. W.; Kavukcuoglu,
736 K.; Kohli, P.; Hassabis, D. Highly Accurate Protein Structure Prediction with AlphaFold.
737 *Nature* **2021**, 596 (7873), 583–589. <https://doi.org/10.1038/s41586-021-03819-2>.
- 738 (51) 14th Community Wide Experiment on the Critical Assessment of Techniques for Protein
739 Structure Prediction <https://predictioncenter.org/casp14/index.cgi> (accessed Jan 18, 2022).
- 740 (52) Kim, Y.; Lovell, S.; Tiew, K.-C.; Mandadapu, S. R.; Alliston, K. R.; Battaile, K. P.; Groutas,
741 W. C.; Chang, K.-O. Broad-Spectrum Antivirals against 3C or 3C-Like Proteases of
742 Picornaviruses, Noroviruses, and Coronaviruses. *J. Virol.* **2012**, 86 (21), 11754–11762.
743 <https://doi.org/10.1128/jvi.01348-12>.
- 744 (53) Hillisch, A.; Pineda, L. F.; Hilgenfeld, R. Utility of Homology Models in the Drug
745 Discovery Process. *Drug Discov. Today* **2004**, 9 (15), 659–669.
746 [https://doi.org/10.1016/S1359-6446\(04\)03196-4](https://doi.org/10.1016/S1359-6446(04)03196-4).
- 747 (54) Anand, K. Coronavirus Main Proteinase (3CLpro) Structure: Basis for Design of Anti-
748 SARS Drugs. *Science* (80-.). **2003**, 300 (5626), 1763–1767.
749 <https://doi.org/10.1126/science.1085658>.

- 750 (55) Yang, H.; Bartlam, M.; Rao, Z. Drug Design Targeting the Main Protease, the Achilles Heel
751 of Coronaviruses. *Curr. Pharm. Des.* **2006**, *12* (35), 4573–4590.
752 <https://doi.org/10.2174/138161206779010369>.
- 753 (56) Boras, B.; Jones, R. M.; Anson, B. J.; Arenson, D.; Aschenbrenner, L.; Bakowski, M. A.;
754 Beutler, N.; Binder, J.; Chen, E.; Eng, H.; Hammond, J.; Hoffman, R.; Kadar, E. P.; Kania,
755 R.; Kimoto, E.; Kirkpatrick, M. G.; Lanyon, L.; Lendy, E. K.; Lillis, J. R.; Luthra, S. A.;
756 Ma, C.; Noell, S.; Obach, R. S.; O'Brien, M. N.; O'Connor, R.; Ogilvie, K.; Owen, D.;
757 Pettersson, M.; Reese, M. R.; Rogers, T.; Rossulek, M. I.; Sathish, J. G.; Stepan, C.;
758 Ticehurst, M.; Updyke, L. W.; Zhu, Y.; Wang, J.; Chatterjee, A. K.; Mesecar, A. D.;
759 Anderson, A. S.; Allerton, C. Discovery of a Novel Inhibitor of Coronavirus 3CL Protease
760 as a Clinical Candidate for the Potential Treatment of COVID-19. *bioRxiv Prepr. Serv.*
761 *Biol.* **2020**. <https://doi.org/10.1101/2020.09.12.293498>.
- 762 (57) Taylor, N. P. Pfizer, in a rare COVID-19 setback, dumps Paxlovid's intravenous sibling in
763 further blow to ACTIV-3 [https://www.fiercebiotech.com/biotech/pfizer-a-rare-covid-19-](https://www.fiercebiotech.com/biotech/pfizer-a-rare-covid-19-setback-dumps-paxlovid-s-intravenous-sibling-to-leave-activ-3-future)
764 [setback-dumps-paxlovid-s-intravenous-sibling-to-leave-activ-3-future](https://www.fiercebiotech.com/biotech/pfizer-a-rare-covid-19-setback-dumps-paxlovid-s-intravenous-sibling-to-leave-activ-3-future) (accessed Mar 6,
765 2022).
- 766 (58) Kocic, G.; Hillen, H. S.; Tegunov, D.; Dienemann, C.; Seitz, F.; Schmitzova, J.; Farnung,
767 L.; Siewert, A.; Höbartner, C.; Cramer, P. Mechanism of SARS-CoV-2 Polymerase Stalling
768 by Remdesivir. *Nat. Commun.* **2021**, *12* (1), 279. [https://doi.org/10.1038/s41467-020-](https://doi.org/10.1038/s41467-020-20542-0)
769 [20542-0](https://doi.org/10.1038/s41467-020-20542-0).
- 770 (59) Beigel, J. H.; Tomashek, K. M.; Dodd, L. E.; Mehta, A. K.; Zingman, B. S.; Kalil, A. C.;
771 Hohmann, E.; Chu, H. Y.; Luetkemeyer, A.; Kline, S.; Lopez de Castilla, D.; Finberg, R.
772 W.; Dierberg, K.; Tapson, V.; Hsieh, L.; Patterson, T. F.; Paredes, R.; Sweeney, D. A.;
773 Short, W. R.; Touloumi, G.; Lye, D. C.; Ohmagari, N.; Oh, M.; Ruiz-Palacios, G. M.;
774 Benfield, T.; Fätkenheuer, G.; Kortepeter, M. G.; Atmar, R. L.; Creech, C. B.; Lundgren,
775 J.; Babiker, A. G.; Pett, S.; Neaton, J. D.; Burgess, T. H.; Bonnett, T.; Green, M.; Makowski,
776 M.; Osinusi, A.; Nayak, S.; Lane, H. C. Remdesivir for the Treatment of Covid-19 — Final
777 Report. *N. Engl. J. Med.* **2020**, *383* (19), 1813–1826.
778 <https://doi.org/10.1056/NEJMoa2007764>.
- 779 (60) Xu, J.; Xue, Y.; Zhou, R.; Shi, P.-Y.; Li, H.; Zhou, J. Drug Repurposing Approach to
780 Combating Coronavirus: Potential Drugs and Drug Targets. *Med. Res. Rev.* **2021**, *41* (3),
781 1375–1426. <https://doi.org/10.1002/med.21763>.
- 782 (61) Saijo, M.; Morikawa, S.; Fukushi, S.; Mizutani, T.; Hasegawa, H.; Nagata, N.; Iwata, N.;
783 Kurane, I. Inhibitory Effect of Mizoribine and Ribavirin on the Replication of Severe Acute
784 Respiratory Syndrome (SARS)-Associated Coronavirus. *Antiviral Res.* **2005**, *66* (2–3),
785 159–163. <https://doi.org/10.1016/j.antiviral.2005.01.003>.
- 786 (62) Chen, F.; Chan, K. .; Jiang, Y.; Kao, R. Y. .; Lu, H. .; Fan, K. .; Cheng, V. C. .; Tsui, W. H.
787 .; Hung, I. F. .; Lee, T. S. . In Vitro Susceptibility of 10 Clinical Isolates of SARS
788 Coronavirus to Selected Antiviral Compounds. *J. Clin. Virol.* **2004**, *31* (1), 69–75.
789 <https://doi.org/10.1016/j.jcv.2004.03.003>.
- 790 (63) Kim, Y.; Lee, C. Ribavirin Efficiently Suppresses Porcine Nidovirus Replication. *Virus Res.*
791 **2013**, *171* (1), 44–53. <https://doi.org/10.1016/j.virusres.2012.10.018>.

- 792 (64) Edwards, C. E.; Yount, B. L.; Graham, R. L.; Leist, S. R.; Hou, Y. J.; Dinnon, K. H.; Sims,
793 A. C.; Swanstrom, J.; Gully, K.; Scobey, T. D.; Cooley, M. R.; Currie, C. G.; Randell, S.
794 H.; Baric, R. S. Swine Acute Diarrhea Syndrome Coronavirus Replication in Primary
795 Human Cells Reveals Potential Susceptibility to Infection. *Proc. Natl. Acad. Sci.* **2020**, *117*
796 (43), 26915–26925. <https://doi.org/10.1073/pnas.2001046117>.
- 797 (65) Choy, K.-T.; Wong, A. Y.-L.; Kaewpreedee, P.; Sia, S. F.; Chen, D.; Hui, K. P. Y.; Chu, D.
798 K. W.; Chan, M. C. W.; Cheung, P. P.-H.; Huang, X.; Peiris, M.; Yen, H.-L. Remdesivir,
799 Lopinavir, Emetine, and Homoharringtonine Inhibit SARS-CoV-2 Replication in Vitro.
800 *Antiviral Res.* **2020**, *178* (March), 104786. <https://doi.org/10.1016/j.antiviral.2020.104786>.
- 801 (66) Brown, A. J.; Won, J. J.; Graham, R. L.; Dinnon, K. H.; Sims, A. C.; Feng, J. Y.; Cihlar, T.;
802 Denison, M. R.; Baric, R. S.; Sheahan, T. P. Broad Spectrum Antiviral Remdesivir Inhibits
803 Human Endemic and Zoonotic Deltacoronaviruses with a Highly Divergent RNA
804 Dependent RNA Polymerase. *Antiviral Res.* **2019**, *169* (January), 104541.
805 <https://doi.org/10.1016/j.antiviral.2019.104541>.
- 806 (67) de Wit, E.; Feldmann, F.; Cronin, J.; Jordan, R.; Okumura, A.; Thomas, T.; Scott, D.; Cihlar,
807 T.; Feldmann, H. Prophylactic and Therapeutic Remdesivir (GS-5734) Treatment in the
808 Rhesus Macaque Model of MERS-CoV Infection. *Proc. Natl. Acad. Sci.* **2020**, *117* (12),
809 6771–6776. <https://doi.org/10.1073/pnas.1922083117>.
- 810 (68) Imran, M.; Alshrari, A. S.; Asdaq, S. M. B.; Abida. Trends in the Development of
811 Remdesivir Based Inventions against COVID-19 and Other Disorders: A Patent Review. *J.*
812 *Infect. Public Health* **2021**, *14* (8), 1075–1086. <https://doi.org/10.1016/j.jiph.2021.06.013>.
- 813 (69) Jeon, S.; Ko, M.; Lee, J.; Choi, I.; Byun, S. Y.; Park, S.; Shum, D.; Kim, S. Identification
814 of Antiviral Drug Candidates against SARS-CoV-2 from FDA-Approved Drugs.
815 *Antimicrob. Agents Chemother.* **2020**, *64* (7). <https://doi.org/10.1128/AAC.00819-20>.
- 816 (70) Bassendine, M. F.; Bridge, S. H.; McCaughan, G. W.; Gorrell, M. D. COVID-19 and
817 Comorbidities: A Role for Dipeptidyl Peptidase 4 (DPP4) in Disease Severity? *J. Diabetes*
818 **2020**, *12* (9), 649–658. <https://doi.org/10.1111/1753-0407.13052>.
- 819 (71) Sharif-Yakan, A.; Kanj, S. S. Emergence of MERS-CoV in the Middle East: Origins,
820 Transmission, Treatment, and Perspectives. *PLoS Pathog.* **2014**, *10* (12), e1004457.
821 <https://doi.org/10.1371/journal.ppat.1004457>.
- 822 (72) Wang, M.; Cao, R.; Zhang, L.; Yang, X.; Liu, J.; Xu, M.; Shi, Z.; Hu, Z.; Zhong, W.; Xiao,
823 G. Remdesivir and Chloroquine Effectively Inhibit the Recently Emerged Novel
824 Coronavirus (2019-NCoV) in Vitro. *Cell Res.* **2020**, No. January, 2019–2021.
825 <https://doi.org/10.1038/s41422-020-0282-0>.
- 826 (73) Zhao, J.; Guo, S.; Yi, D.; Li, Q.; Ma, L.; Zhang, Y.; Wang, J.; Li, X.; Guo, F.; Lin, R.;
827 Liang, C.; Liu, Z.; Cen, S. A Cell-Based Assay to Discover Inhibitors of SARS-CoV-2 RNA
828 Dependent RNA Polymerase. *Antiviral Res.* **2021**, *190*, 105078.
829 <https://doi.org/10.1016/j.antiviral.2021.105078>.
- 830 (74) Sheahan, T. P.; Sims, A. C.; Zhou, S.; Graham, R. L.; Pruijssers, A. J.; Agostini, M. L.;
831 Leist, S. R.; Schäfer, A.; Dinnon, K. H.; Stevens, L. J.; Chappell, J. D.; Lu, X.; Hughes, T.
832 M.; George, A. S.; Hill, C. S.; Montgomery, S. A.; Brown, A. J.; Bluemling, G. R.; Natchus,

- 833 M. G.; Saindane, M.; Kolykhalov, A. A.; Painter, G.; Harcourt, J.; Tamin, A.; Thornburg,
834 N. J.; Swanstrom, R.; Denison, M. R.; Baric, R. S. An Orally Bioavailable Broad-Spectrum
835 Antiviral Inhibits SARS-CoV-2 in Human Airway Epithelial Cell Cultures and Multiple
836 Coronaviruses in Mice. *Sci. Transl. Med.* **2020**, *12* (541), eabb5883.
837 <https://doi.org/10.1126/scitranslmed.abb5883>.
- 838 (75) Lin, M.-H.; Moses, D. C.; Hsieh, C.-H.; Cheng, S.-C.; Chen, Y.-H.; Sun, C.-Y.; Chou, C.-
839 Y. Disulfiram Can Inhibit MERS and SARS Coronavirus Papain-like Proteases via
840 Different Modes. *Antiviral Res.* **2018**, *150* (August 2017), 155–163.
841 <https://doi.org/10.1016/j.antiviral.2017.12.015>.
- 842 (76) Armstrong, L. A.; Lange, S. M.; Dee Cesare, V.; Matthews, S. P.; Nirujogi, R. S.; Cole, I.;
843 Hope, A.; Cunningham, F.; Toth, R.; Mukherjee, R.; Bojkova, D.; Gruber, F.; Gray, D.;
844 Wyatt, P. G.; Cinatl, J.; Dikic, I.; Davies, P.; Kulathu, Y. Biochemical Characterization of
845 Protease Activity of Nsp3 from SARS-CoV-2 and Its Inhibition by Nanobodies. *PLoS One*
846 **2021**, *16* (7), e0253364. <https://doi.org/10.1371/journal.pone.0253364>.
- 847 (77) F, K.; S, M.; M, K.; T, H.; H, K.; M, T. Antiviral Activities of Mycophenolic Acid and
848 IMD-0354 against SARS-CoV-2. *Microbiol. Immunol.* **2020**, *64* (9), 635–639.
849 <https://doi.org/10.1111/1348-0421.12828>.
- 850 (78) Chan, J. F. W.; Chan, K.-H.; Kao, R. Y. T.; To, K. K. W.; Zheng, B.-J.; Li, C. P. Y.; Li, P.
851 T. W.; Dai, J.; Mok, F. K. Y.; Chen, H.; Hayden, F. G.; Yuen, K.-Y. Broad-Spectrum
852 Antivirals for the Emerging Middle East Respiratory Syndrome Coronavirus. *J. Infect.*
853 **2013**, *67* (6), 606–616. <https://doi.org/10.1016/j.jinf.2013.09.029>.
- 854 (79) Jan, J.-T.; Cheng, T.-J. R.; Juang, Y.-P.; Ma, H.-H.; Wu, Y.-T.; Yang, W.-B.; Cheng, C.-
855 W.; Chen, X.; Chou, T.-H.; Shie, J.-J.; Cheng, W.-C.; Chein, R.-J.; Mao, S.-S.; Liang, P.-
856 H.; Ma, C.; Hung, S.-C.; Wong, C.-H. Identification of Existing Pharmaceuticals and Herbal
857 Medicines as Inhibitors of SARS-CoV-2 Infection. *Proc. Natl. Acad. Sci.* **2021**, *118* (5),
858 e2021579118. <https://doi.org/10.1073/pnas.2021579118>.
- 859 (80) Cheng, K.-W.; Cheng, S.-C.; Chen, W.-Y.; Lin, M.-H.; Chuang, S.-J.; Cheng, I.-H.; Sun,
860 C.-Y.; Chou, C.-Y. Thiopurine Analogs and Mycophenolic Acid Synergistically Inhibit the
861 Papain-like Protease of Middle East Respiratory Syndrome Coronavirus. *Antiviral Res.*
862 **2015**, *115*, 9–16. <https://doi.org/10.1016/j.antiviral.2014.12.011>.
- 863 (81) Chou, C.-Y.; Chien, C.-H.; Han, Y.-S.; Prebanda, M. T.; Hsieh, H.-P.; Turk, B.; Chang, G.-
864 G.; Chen, X. Thiopurine Analogues Inhibit Papain-like Protease of Severe Acute
865 Respiratory Syndrome Coronavirus. *Biochem. Pharmacol.* **2008**, *75* (8), 1601–1609.
866 <https://doi.org/10.1016/j.bcp.2008.01.005>.
- 867 (82) Swaim, C. D.; Perng, Y.-C.; Zhao, X.; Canadeo, L. A.; Harastani, H. H.; Darling, T. L.;
868 Boon, A. C. M.; Lenschow, D. J.; Huijbregtse, J. M. 6-Thioguanine Blocks SARS-CoV-2
869 Replication by Inhibition of PLpro Protease Activities. *bioRxiv* **2020**, 2020.07.01.183020.
870 <https://doi.org/10.1101/2020.07.01.183020>.
- 871 (83) de Wilde, A. H.; Jochmans, D.; Posthuma, C. C.; Zevenhoven-Dobbe, J. C.; van
872 Nieuwkoop, S.; Bestebroer, T. M.; van den Hoogen, B. G.; Neyts, J.; Snijder, E. J. Screening
873 of an FDA-Approved Compound Library Identifies Four Small-Molecule Inhibitors of

- 874 Middle East Respiratory Syndrome Coronavirus Replication in Cell Culture. *Antimicrob.*
875 *Agents Chemother.* **2014**, 58 (8), 4875–4884. <https://doi.org/10.1128/AAC.03011-14>.
- 876 (84) Theerawatanasirikul, S.; Kuo, C. J.; Phetcharat, N.; Lekcharoensuk, P. In Silico and in Vitro
877 Analysis of Small Molecules and Natural Compounds Targeting the 3CL Protease of Feline
878 Infectious Peritonitis Virus. *Antiviral Res.* **2020**, 174, 104697.
879 <https://doi.org/10.1016/j.antiviral.2019.104697>.
- 880 (85) Xu, Z.; Yao, H.; Shen, J.; Wu, N.; Xu, Y.; Lu, X.; Zhu, W.; Li, L.-J. Nelfinavir Is Active
881 Against SARS-CoV-2 in Vero E6 Cells. *ChemRxiv Prepr. Serv. Chem.* **2020**.
882 <https://doi.org/10.26434/CHEMRXIV.12039888.V1>.
- 883 (86) Yamamoto, N.; Yang, R.; Yoshinaka, Y.; Amari, S.; Nakano, T.; Cinatl, J.; Rabenau, H.;
884 Doerr, H. W.; Hunsmann, G.; Otaka, A.; Tamamura, H.; Fujii, N.; Yamamoto, N. HIV
885 Protease Inhibitor Nelfinavir Inhibits Replication of SARS-Associated Coronavirus.
886 *Biochem. Biophys. Res. Commun.* **2004**, 318 (3), 719–725.
887 <https://doi.org/10.1016/j.bbrc.2004.04.083>.
- 888 (87) Ma, C.; Sacco, M. D.; Hurst, B.; Townsend, J. A.; Hu, Y.; Szeto, T.; Zhang, X.; Tarbet, B.;
889 Marty, M. T.; Chen, Y.; Wang, J. Boceprevir, GC-376, and Calpain Inhibitors II, XII Inhibit
890 SARS-CoV-2 Viral Replication by Targeting the Viral Main Protease. *Cell Res.* **2020**, 30
891 (8), 678–692. <https://doi.org/10.1038/s41422-020-0356-z>.
- 892 (88) Hu, Y.; Ma, C.; Szeto, T.; Hurst, B.; Tarbet, B.; Wang, J. Boceprevir, Calpain Inhibitors II
893 and XII, and GC-376 Have Broad-Spectrum Antiviral Activity against Coronaviruses in
894 Cell Culture. *bioRxiv* **2020**. <https://doi.org/10.1101/2020.10.30.362335>.
- 895 (89) Fu, L.; Ye, F.; Feng, Y.; Yu, F.; Wang, Q.; Wu, Y.; Zhao, C.; Sun, H.; Huang, B.; Niu, P.;
896 Song, H.; Shi, Y.; Li, X.; Tan, W.; Qi, J.; Gao, G. F. Both Boceprevir and GC376
897 Efficaciously Inhibit SARS-CoV-2 by Targeting Its Main Protease. *Nat. Commun.* **2020**, 11
898 (1), 4417. <https://doi.org/10.1038/s41467-020-18233-x>.
- 899 (90) Kim, Y.; Lovell, S.; Tiew, K.-C.; Mandadapu, S. R.; Alliston, K. R.; Battaile, K. P.; Groutas,
900 W. C.; Chang, K.-O. Broad-Spectrum Antivirals against 3C or 3C-Like Proteases of
901 Picornaviruses, Noroviruses, and Coronaviruses. *J. Virol.* **2012**, 86 (21), 11754–11762.
902 <https://doi.org/10.1128/JVI.01348-12>.
- 903 (91) Kim, Y.; Liu, H.; Galasiti Kankanamalage, A. C.; Weerasekara, S.; Hua, D. H.; Groutas,
904 W. C.; Chang, K.-O.; Pedersen, N. C. Reversal of the Progression of Fatal Coronavirus
905 Infection in Cats by a Broad-Spectrum Coronavirus Protease Inhibitor. *PLOS Pathog.* **2016**,
906 12 (3), e1005531. <https://doi.org/10.1371/journal.ppat.1005531>.
- 907 (92) Chen, L.; Gui, C.; Luo, X.; Yang, Q.; Günther, S.; Scandella, E.; Drosten, C.; Bai, D.; He,
908 X.; Ludewig, B.; Chen, J.; Luo, H.; Yang, Y.; Yang, Y.; Zou, J.; Thiel, V.; Chen, K.; Shen,
909 J.; Shen, X.; Jiang, H. Cinanserin Is an Inhibitor of the 3C-Like Proteinase of Severe Acute
910 Respiratory Syndrome Coronavirus and Strongly Reduces Virus Replication In Vitro. *J.*
911 *Virol.* **2005**, 79 (11), 7095–7103. <https://doi.org/10.1128/JVI.79.11.7095-7103.2005>.
- 912 (93) Benoni, R.; Krafcikova, P.; Baranowski, M. R.; Kowalska, J.; Boura, E.; Cahova, H.
913 Substrate Specificity of SARS-CoV-2 Nsp10-Nsp16 Methyltransferase Roberto. *bioRxiv*
914 *Prepr. Serv. Biol.* **2020**, 21 (1), 1–9. <https://doi.org/10.1101/2020.07.30.228478>.

- 915 (94) Perveen, S.; Khalili Yazdi, A.; Devkota, K.; Li, F.; Ghiabi, P.; Hajian, T.; Loppnau, P.;
916 Bolotokova, A.; Vedadi, M. A High-Throughput RNA Displacement Assay for Screening
917 SARS-CoV-2 Nsp10-Nsp16 Complex toward Developing Therapeutics for COVID-19.
918 *SLAS Discov. Adv. Sci. Drug Discov.* **2021**, 247255522098504.
919 <https://doi.org/10.1177/2472555220985040>.
- 920 (95) Aouadi, W.; Blanjoie, A.; Vasseur, J.; Debart, F.; Canard, B.; Decroly, E. Binding of the
921 Methyl Donor S²-Adenosyl-1-Methionine to Middle East Respiratory Syndrome
922 Coronavirus 2'-O-Methyltransferase Nsp16 Promotes Recruitment of the Allosteric
923 Activator Nsp10. *J. Virol.* **2017**, 91 (5), 1–18. <https://doi.org/10.1128/JVI.02217-16>.
- 924 (96) Decroly, E.; Debarnot, C.; Ferron, F.; Bouvet, M.; Coutard, B.; Imbert, I.; Gluais, L.;
925 Papageorgiou, N.; Sharff, A.; Bricogne, G.; Ortiz-Lombardia, M.; Lescar, J.; Canard, B.
926 Crystal Structure and Functional Analysis of the SARS-Coronavirus RNA Cap 2'-O-
927 Methyltransferase Nsp10/Nsp16 Complex. *PLoS Pathog.* **2011**, 7 (5), e1002059.
928 <https://doi.org/10.1371/journal.ppat.1002059>.
- 929 (97) Bouvet, M.; Debarnot, C.; Imbert, I.; Selisko, B.; Snijder, E. J.; Canard, B.; Decroly, E. In
930 Vitro Reconstitution of SARS-Coronavirus MRNA Cap Methylation. *PLoS Pathog.* **2010**,
931 6 (4), e1000863. <https://doi.org/10.1371/journal.ppat.1000863>.
- 932 (98) Muratov, E.; Zakharov, A. Viribus Unitis: Drug Combinations as a Treatment Against
933 COVID-19. *ChemRxiv Prepr. Serv. Chem.* **2020**.
934 <https://doi.org/10.26434/chemrxiv.12143355.v1> DOI: 10.26434/chemrxiv.12143355.v1.
- 935 (99) Yazdani, S.; Maio, N. De; Ding, Y.; Shahani, V.; Goldman, N.; Schapira, M. Genetic
936 Variability of the SARS-CoV-2 Pocketome. *J. Proteome Res.* **2021**, 20, 4215.
937 <https://doi.org/10.1021/ACS.JPROTEOME.1C00206>.
- 938 (100) Cho, E.; Rosa, M.; Anjum, R.; Mehmood, S.; Soban, M.; Mujtaba, M.; Bux, K.; Moin, S.
939 T.; Tanweer, M.; Dantu, S.; Pandini, A.; Yin, J.; Ma, H.; Ramanathan, A.; Islam, B.; Mey,
940 A. S. J. S.; Bhowmik, D.; Haider, S. Dynamic Profiling of β -Coronavirus 3CL M pro
941 Protease Ligand-Binding Sites. *J. Chem. Inf. Model.* **2021**, 61 (6), 3058–3073.
942 <https://doi.org/10.1021/acs.jcim.1c00449>.
- 943 (101) Yoon, J.; Kim, G.; Jarhad, D. B.; Kim, H.-R.; Shin, Y.-S.; Qu, S.; Sahu, P. K.; Kim, H. O.;
944 Lee, H. W.; Wang, S. Bin; Kong, Y. J.; Chang, T.-S.; Ogando, N. S.; Kovacicova, K.;
945 Snijder, E. J.; Posthuma, C. C.; van Hemert, M. J.; Jeong, L. S. Design, Synthesis, and Anti-
946 RNA Virus Activity of 6'-Fluorinated-Aristeromycin Analogues. *J. Med. Chem.* **2019**, 62
947 (13), 6346–6362. <https://doi.org/10.1021/acs.jmedchem.9b00781>.
- 948 (102) Lee, H.; Ren, J.; Pesavento, R. P.; Ojeda, I.; Rice, A. J.; Lv, H.; Kwon, Y.; Johnson, M. E.
949 Identification and Design of Novel Small Molecule Inhibitors against MERS-CoV Papain-
950 like Protease via High-Throughput Screening and Molecular Modeling. *Bioorg. Med.*
951 *Chem.* **2019**, 27 (10), 1981–1989. <https://doi.org/10.1016/j.bmc.2019.03.050>.
- 952 (103) *Identification of Inhibitors of SARS-Cov2 M-Pro Enzymatic Activity Using a Small*
953 *Molecule Repurposing Screen*; 2021. <https://doi.org/10.6019/CHEMBL4495564>.
- 954 (104) Prichard, M. N. New Approaches to Antiviral Drug Discovery (Genomics/Proteomics). In
955 *Human Herpesviruses Biology, Therapy, and Immunoprophylaxis*; Arvin, A., Campadelli-

- 956 Fiume, G., Mocarski, E., Moore, P. S., Roizman, B., Whitley, R., Yamanishi, K., Eds.;
957 Cambridge, 2007.
- 958 (105) Muratov, E. N.; Amaro, R.; Andrade, C. H.; Brown, N.; Ekins, S.; Fourches, D.; Isayev, O.;
959 Kozakov, D.; Medina-Franco, J. L.; Merz, K. M.; Oprea, T. I.; Poroikov, V.; Schneider, G.;
960 Todd, M. H.; Varnek, A.; Winkler, D. A.; Zakharov, A. V.; Cherkasov, A.; Tropsha, A. A
961 Critical Overview of Computational Approaches Employed for COVID-19 Drug
962 Discovery. *Chem. Soc. Rev.* **2021**, *50* (16), 9121–9151. <https://doi.org/10.1039/d0cs01065k>.
- 963 (106) Grange, Z. L.; Goldstein, T.; Johnson, C. K.; Anthony, S.; Gilardi, K.; Daszak, P.; Olival,
964 K. J.; O'Rourke, T.; Murray, S.; Olson, S. H.; Togami, E.; Vidal, G.; Mazet, J. A. K.
965 Ranking the Risk of Animal-to-Human Spillover for Newly Discovered Viruses. *Proc. Natl.*
966 *Acad. Sci.* **2021**, *118* (15), e2002324118. <https://doi.org/10.1073/pnas.2002324118>.
- 967 (107) Spillover <https://spillover.global/ranking-comparison/> (accessed Aug 12, 2021).
- 968 (108) Antiviral Program for Pandemics. <https://ncats.nih.gov/antivirals> (accessed Sep 7, 2021).
- 969 (109) The Rapidly Emerging Antiviral Drug Development Initiative (READDI).
970 <https://www.readdi.org/> (accessed Sep 7, 2021).
- 971 (110) Open science drug discovery partnership, READDI, aims to invest \$125 million to prevent
972 future pandemics [https://pharmacy.unc.edu/2020/04/open-science-drug-discovery-](https://pharmacy.unc.edu/2020/04/open-science-drug-discovery-partnership-readdi-aims-to-invest-125-million-to-prevent-future-pandemics/)
973 [partnership-readdi-aims-to-invest-125-million-to-prevent-future-pandemics/](https://pharmacy.unc.edu/2020/04/open-science-drug-discovery-partnership-readdi-aims-to-invest-125-million-to-prevent-future-pandemics/) (accessed Feb
974 2, 2021).
- 975 (111) da Costa, V. G.; Moreli, M. L.; Saivish, M. V. The Emergence of SARS, MERS and Novel
976 SARS-2 Coronaviruses in the 21st Century. *Arch. Virol.* **2020**, *165* (7), 1517–1526.
977 <https://doi.org/10.1007/s00705-020-04628-0>.
- 978 (112) Bobrowski, T.; Chen, L.; Eastman, R. T.; Itkin, Z.; Shinn, P.; Chen, C. Z.; Guo, H.; Zheng,
979 W.; Michael, S.; Simeonov, A.; Hall, M. D.; Zakharov, A. V.; Muratov, E. N. Synergistic
980 and Antagonistic Drug Combinations against SARS-CoV-2. *Mol. Ther.* **2021**, *29* (2), 873–
981 885. <https://doi.org/10.1016/j.ymthe.2020.12.016>.
- 982 (113) Dutta, K. Allosteric Site of ACE-2 as a Drug Target for COVID-19. *ACS Pharmacol.*
983 *Transl. Sci.* **2022**, acsptsci.2c00003. <https://doi.org/10.1021/acsptsci.2c00003>.
- 984

Conservation analysis of sequence and structure of key coronavirus proteins supports the discovery of broad-spectrum antiviral medications.

Cleber C. Melo-Filho, Tesia Bobrowski,

Holli-Joi Sullivan, Zoe Sessions,

Konstantin Popov, Nathaniel J. Moorman,

Ralph Baric, Eugene Muratov,* Alexander

Tropsha.*

